AD-A116 109 FRAUNHOFER-GESELLSCHAFT GARMISCH-PARTENKIRCHEN (GERMA--ETC F/G 20/6
ATMOSPHERIC CONDITIONS INFLUENCING SLANT PATH LOW VISIBILITY.(U)
JAN 82 R REITER, W CARNUTH, R SLADKOVIC DAJA37-80-C-0345

UNCLASSIFIED NL

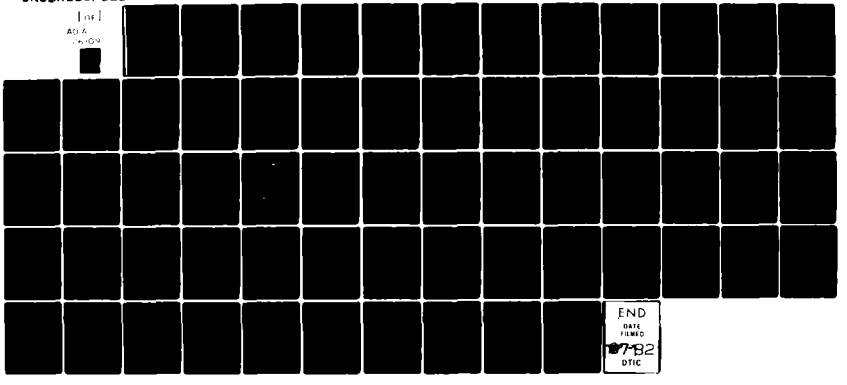

END
DATE FILMED
7-82
DTIC

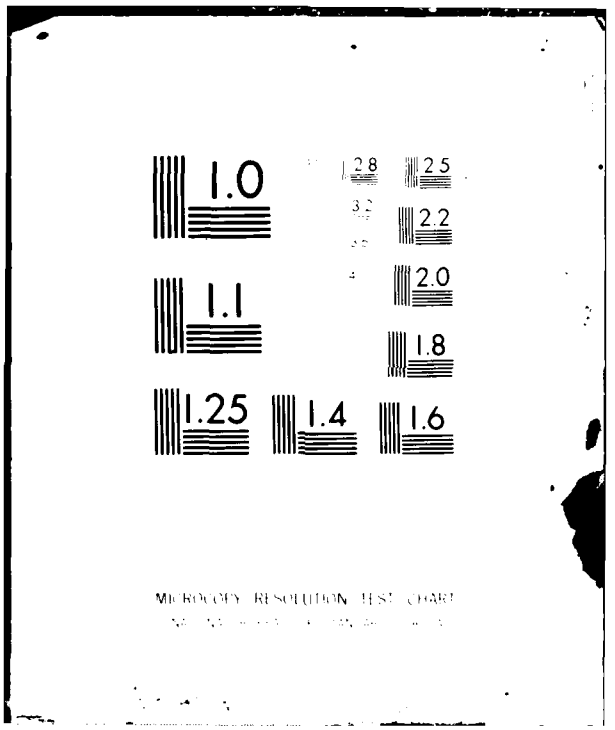
1.0
2.8
2.5
2.2
2.0
1.1
1.8
1.25
1.4
1.6
MICROCOPY RESOLUTION TEST CHART

AD_____

(3)

ATMOSPHERIC CONDITIONS INFLUENCING SLANT PATH LOW VISIBILITY

Fourth Interim Report

by

Reinhold Reiter
Walter Carnuth
Rudolf Sladkovic
Werner Funk

January 1982

EUROPEAN RESEARCH OFFICE
United States Army
London England

Contract Number DAJA37-80-C-0345

Fraunhofer Institut für Atmosphärische
Umweltforschung
Kreuzeckbahnstrasse 19
D-8100 Garmisch-Partenkirchen

UNCLASSIFIED

SECURITY CLASSIFICATION OF THIS PAGE (When Data Entered)

REPORT DOCUMENTATION PAGE		READ INSTRUCTIONS BEFORE COMPLETING FORM
1. REPORT NUMBER	2. GOVT ACCESSION NO. AD-A116	3. RECIPIENT'S CATALOG NUMBER 709
4. TITLE (and Subtitle) Atmospheric Conditions Influencing Slant Path Low Visibility		5. TYPE OF REPORT & PERIOD COVERED Interim Report Sept 81 - Jan 82
		6. PERFORMING ORG. REPORT NUMBER
7. AUTHOR(s) Reinhold Reiter, Walter Carnuth, Rudolf Sladkovic Werner Funk		8. CONTRACT OR GRANT NUMBER(s) DAJA37-80-C-0345
9. PERFORMING ORGANIZATION NAME AND ADDRESS Fraunhofer Institut für Atmosphärische Umweltforschung, Kreuzeckbahnstrasse 19 D-8100 Garmisch-Partenkirchen, West Germany		10. PROGRAM ELEMENT, PROJECT, TASK AREA & WORK UNIT NUMBERS 61102A IT161102BH57-01
11. CONTROLLING OFFICE NAME AND ADDRESS USARDSG-UK Box 65, FPO New York, NY 09510		12. REPORT DATE January 1982
		13. NUMBER OF PAGES 41 plus Tab.1-9,Fig.1-8
14. MONITORING AGENCY NAME & ADDRESS(if different from Controlling Office)		15. SECURITY CLASS. (of this report) Unclassified
		15a. DECLASSIFICATION/DOWNGRADING SCHEDULE

16. DISTRIBUTION STATEMENT (of this Report)

Approved for public release; Distribution unlimited

17. DISTRIBUTION STATEMENT (of the abstract entered in Block 20, if different from Report)

18. SUPPLEMENTARY NOTES

19. KEY WORDS (Continue on reverse side if necessary and identify by block number)

Visibility, optical propagation; optical extinction; slant path; atmospheric propagation; visible light; infra-red.

20. ABSTRACT (Continue on reverse side if necessary and identify by block number)

The report presents results of transmission measurements in the visible and thermal infrared range along a slant path of 2.7 km length and 19° inclination. To infer correlations, all meteorological parameters, visibility, aerosol spectrum are measured at both ends of the path. For monitoring the aerosol distribution along the path serves a four-frequency lidar (ranging between 380 and 1060 nm). Transmissivity and extinction coefficient in VIS and IR are parameterized considering the following quantities: Clouds, mist, haze, aerosols, rate of rainfall, and snowfall.

DD FORM 1 JAN 73 1473 EDITION OF 1 NOV 65 IS OBSOLETE S/N 0102-LF-014-6601

UNCLASSIFIED

SECURITY CLASSIFICATION OF THIS PAGE (When Data Entered)

Table of contents

1. Technical State of the Measuring Systems

1.1. Transmissometer

The Barnes transmissometers for the visible and infrared wavelength ranges worked satisfactorily in the reporting period. Problematic is however now as in the past the short life of the halogen lamps which could not be essentially prolonged through any of the measures taken so far such as retarding of the switch-on and off procedure, permanent heating of the lamp at reduced efficiency while inoperative and so on. Thus, in the first 5 months of the year the lamp had to be replaced no less than 4 times. Since, in all, three source assemblies are available which after lamp failure are always sent immediately to the German representative of Barnes for free but time-consuming new equipment, it was till now always possible to keep the system ready for operation. Choice of the measuring dates had, of course, to be made with some care to avoid if ever possible idle motion with poorly usable results. In the meantime, however,there are prospects for solving the problem since we succeeded in locating the lamp type and a source of supply in the Federal Republic of Germany. We found out that replacement of the lamps does not pose any problems and can be carried out without readjustment of the lamp. The only remaining problem is calibration which can however be solved through either an improvised close-up method or in the previous manner through calibration measurements at high atmospheric transmission. We are also about checking whether the modification on the Barnes unit for which drawings have been kindly sent to us from ASL can be made in our own shop.

1.2. Measuring station for meteorological data at the Kreuzeck

In February, the station was extended by an anemometer. A previously procured Ruppersberg visibility recorder is for comparison purposes still operating at the Institute but will be installed at the Kreuzeck shortly. Transmission of all data via telemetry is running troublefree. Short-term failures, mentioned in the preceding report, could be eliminated in the meantime.

1.3. Lidars

Both lidar systems worked troublefree in the reporting period. On the mobile lidar, efforts for using the 1060 nm wavelength have been continued. Since the S-1 photomultiplier we bought last year did not deliver quite ideal results, it seemed appropriate to pursue the alternative possibility of the semi-conductor detector (PIN-diode). A complete measuring head consisting of a YAG 444 photodiode, amplifier and power supply which was kindly lent to us by DFVLR delivered very good results - at least for the 1060 and 694 nm wavelengths. A similar measuring head has been constructed in the meantime and is being checked. In doing so it will be tried through selection of a photodiode with other spectral sensitivity to detect also the 530 and 347 nm wavelengths without a detector change becoming necessary during the measurements.

2. Compilation of Transmissometer Measurements Since February 1981

2.1. 25 February 1981, 10.00 - 16.00 CET

The weather situation is almost the same as on 23.02.81 (last measurements in the 3rd Interim Report). Early in the morning, with short-time NE-wind, a flat ground fog layer flows in. It remains however weak along the measuring path and dissolves again at 11.00 h, i.e. before reaching the nominal temperature of the IR radiation source. A flat haze layer with high concentration is left. At 11.00 h, the valley wind develops again. Initially the top of the haze layer rises again and later, at 13.45 h, a St-sheet, visible already for a longer period at the end of the valley, advances to the measuring site. From 16.00 h there is a closed St-sheet. By means of lidar its base was located at 1080 m while its top extends to 1250 m according to visual observation by our technician at the station Wank (1800 m a.s.l.). In IR, transmission through this layer could still be measured but no longer in the visible range.

2.2. 10 March 1981, 08.00 - 18.43 CET

During the influx of mild, humid and very clear maritime air from SW there was temporarily light precipitation, below 2000 m asl as rain. The bases of Ns and As clouds, respectively, remain then above 2500 m and only thin Cu fra drift for a short time through the measuring path. Although the temporarily occurring rain was clearly perceived in the lidar signals and led to a marked increase of extinction in both channels, a response in the ombrometers was shown neither in the valley nor at the Kreuzeck.

2.3. 11 March 1981, 08.00 - 15.40 CET

Weather conditions were almost identical with those on the previous day. The cloud base remained above 2600 m asl, the measuring path was free from clouds. Again, it rained in the forenoon but with lesser extinction effects than the day before. Nevertheless useful precipitation rates, well to be correlated with the transmission data, are available from both stations. Since it had been raining before the measuring campaign was started, the collecting funnels of the rain gauges were probably still moistened and the response was not delayed as in the case of dry instruments.

2.4. 25 March 1981, 09.00 - 10.00 CET

This measuring series was started during a withdrawing precipitation area but when the nominal temperature of the IR source was reached the rain had already stopped. Shortly thereafter the measurements had to be ceased because of a halogen lamp failure.

2.5. 03 April 1981, 08.00 - 20.36 CET

Gradient-weak easterly weather conditions prevailed within the range of an air mass front between dry-cool air in E and mild air in W. Initially 10 km visibility have been measured in the valley. Later, with developing valley wind, exceptionally high aerosol concentrations are observed similar to those on 28 Feb 80.

Visibility at the ground was reduced to 4 km, the Kreuzeck was hardly visible. However, towards evening with persistent valley wind, air poorer in aerosol was transported in quite atypical manner to the lower layers so that visibility was considerably improved from below. This interesting case is discussed in more detail in Section 3.

2.6. 06 April 1981, 09.00 - 11.00 CET

During this shorter measuring campaign cumulus clouds of varying thickness appeared from time to time in otherwise dominantly fair weather at the mountains and also along the measuring path. After transmission from noon on was reduced to unmeasurable small values the measurements were stopped.

2.7. 21 April 1981, 08.00 - 16.45 CET

This day, a relatively humid air mass of polar-maritime origin prevailed in which moderate, high-reaching and homogeneous haze was observed. During the day cumulus clouds developed but the measuring path was for the most part cloudless. In the early afternoon a weak shower occurred having just little influence on the transmission. The slant lidar profiles show from 10.00 h a homogeneous haze structure along the entire measuring path. Accordingly, the transmissometer curves are running nearly constant in both channels throughout the day.

2.8. 23 April 1981, 09.00 - 17.00 CET

The general weather situation is almost unchanged compared to 21 April. In the existing aged air mass strong haze appears, more distant mountains can no longer be seen. In the early morning the vertical lidar shows a very sharp top of the haze layer at 2100 m a.s.l. The measuring campaign had been started in the expectation that with the valley wind the aerosol concentration would continue to increase but this was not the case. Clouds

formed this day only above 2000 m, the measuring path remained cloudless. Transmission in both ranges changed little during the day.

2.9. 24 April 1981, 08.00 - 13.00 CET

In the morning a closed stratus sheet lay in the valley floor with base at 1200 m a.s.l. which dissolved in the following period as it was to be expected or changed into stratocumulus. Aloft a second stratus layer was recorded at 1800 m. Below the clouds prevailed strong hazy dust. In the course of the forenoon the measuring path became temporarily free and from 08.40 h it was permanently cloudless and so the measurement was stopped after midday.

2.10. 07 May 1981, Calibration measurement during clear air conditions

2.11. 22 May 1981, 08.00 - 16.00 CET

This day, there was a frontal passage with rather heavy precipitation between 11.00 and 17.00 h. During the measuring period fell 9 mm rain. However, the station Kreuzeck was for the most part in clouds which can clearly be seen from the Knollenberg spectra. Therefore, only during a few short periods there was no superposition by cloud and precipitation extinction.

2.12. 16 June 1981, 08.40 - 15.40 CET

This day, too, a passage of a cold front occurred with thundery rain showers. During a first violent shower between 10.20 and 11.00 hs the cloud base lay still far above the Kreuzeck level so that transmission through precipitation could be measured undisturbed. For a short time precipitation rates up to 2 mm/h have been measured in the valley and more than 4 mm/h at the Kreuzeck. A pause of rainfall during which cloudiness developed on the measuring path was followed by another, still more intense shower

with peak rates up to 17 mm/h at the Kreuzeck and more than 9 mm/h in the valley. During this period the measuring path was at least temporarily free. After termination of rainfall and decreasing cloudiness the measuring series was ceased in the afternoon.

2.13. 01 July 1981, 08.30 - 02 July 1981, 08.00 CET

For the first time it was possible this day to carry out a 24-hour measuring series, planned already for a rather long time in order to cover a full daily course of the transmission values. Under the influence of a flat high pressure zone moving from southern Mid-Europe to the east fair weather prevailed with only occasional passages of high-level cloudiness. As it is the rule during such weather situation, a well pronounced mountain-valley-wind system was observed, i.e. strong up-valley blowing winds by day and weaker slope winds at night. The trend of the vertical aerosol structure during the measuring period was well detected through backscatter profiles taken by the two lidar systems at half-hourly intervals. A marked daily variation of the haze layer appeared under the influence of mountain-valley wind and convection. However, the variations were mainly found at levels above 2000 m so that transmission in the visible as well as in the infrared range remained constant. Also visibility reduction during the night hours, indicated by the Ruppersberg visibility meter and caused by humidity increase at falling themperature, did not affect the transmission values. Apparently, such processes take place only in very flat layers. All-day measuring series of this kind will be repeated in the fall and winter half-year because during this period more pronounced daily variations of visibility conditions are to be expected also in the lower layers.

2.14. 22 July 1981, Calibration measurement

2.15. 27 July 1981, 07.00 - 18.00 CET

After a prolonged period of bad weather in which the cloud base

remained mostly under the Kreuzeck level, thus making measurements impossible, this day was suitable for detecting over many hours the decreasing transmission through precipitation alone where despite protracted rainfall thin clouds drifted only for a very short time through the measuring path. With the approach of a warm front from north-west mainly drizzling rain in varying intensity fell from stratiform, relatively high clouds. Although the precipitation rates were so low that the measuring instruments, especially in the valley, were responsive only for a short time (recorded total precipitation rate during the measuring period .48 mm at the Kreuzeck and .22 mm in the valley), a quite considerable reduction of transmission was observed in both channels comparable to the values measured on 6 June at essentially higher precipitation rates. This finding will be disccussed in more detail in the next section.

3. Discussion of Some Typical Results

3.1. Calibration measurements for determining the reference value

As repeatedly mentioned, calibration measurements are made on as haze-free days as possible for determining the reference value, i.e., the value corresponding to 100% transmission in the visible and infrared range. For the infrared, this calibration method can as previously deliver only provisional results since the contribution of molecular absorption to the total extinction is unknown. Although the concentration of the gases to be considered (in the first place water vapor, otherwise CO_2, ozone, hydrocarbons) is known through our measurements, calculation of the extinction is very complicated because of the many absorption lines in the IR-window. For the calculations exists, as is known, the so-called LOWTRAN computer program in different variants and developmental stages, respectively. This program is very extensive and requires a larger computer for operation. Since the complete LOWTRAN 5, written in Fortran, cannot run on our computer and we otherwise do not need all parts of it, we are presently checking

the possibility of rewriting or simplifying the LOWTRAN in a way that it will no longer exceed the capacity of our system.

Independent thereof it was however noted that the reference value in the infrared channel decreased since the end of October 1980 by more than 50%. A reason for this could not be found. All optical components in the receiver system are flawless, as far as this can be located by visual checks, and contaminations on the few elements in the radiation source are equally to be excluded and, what is more, they would make themselves felt more in the visual range. As a possible cause remains, though not very likely, a change of the detector sensitivity and a change of temperature in the blackbody which should be 1000°C. This will be checked by a bolometer in the future. In the infrared channel - despite the frequent lamp replacement - no essential change of the reference value was observed.

3.2. Extinction through different media

3.2.1. Dry aerosol

It has been observed earlier that dry aerosol even in very high concentration reduces but negligibly, if at all, the infrared transmission. In the absence of clouds and precipitation IR levels have been measured which, though not quite constant, are not correlated with the aerosol concentration either. This finding was confirmed.

An example of a diurnal variation of transmission at increasing aerosol concentration on 23.02.1981 is shown by the diagram Fig. 1 in the ANNEX. Versus time are plotted as previously the visual (σ_{VIS}) and infrared (σ_{IR}) extinction coefficients in km^{-1}, for clarity's sake increasing toward the bottom as shown by the linear ordinate scale in the left. If we use the right-hand logarithmic scale for the transmission factor τ in %, the curves represent likewise this quantity. The extinction coefficient is however

the actual physically relevant quantity which we clearly can imagine as the sum of the effective cross-section areas of all extinguishing particles per volume unit. In contrast to τ, σ behaves additively so that here only linear averaging over the time is meaningful.

The correlation between τ and σ is given by Lambert-Beer's law which is here taken as valid - at least approximatively: $\tau = 100 \cdot \exp(-\sigma L)$ where L is the length of the measuring path; σ is, of course, the mean value over the entire measuring path.

We clearly recognize in the diagram the, on an average, sharply increasing tendency of the visible extinction caused by the introduction of heavier polluted air from the pre-alpine region through the usually up-valley blowing wind during the day. By contrast, no such trend is found with the infrared extinction which even decreases a little, probably due to the falling humidity during daytime hours.

Only in one single case we observed during a variation in the aerosol concentration also a change of the infrared transmission. This was on 3 April 1981 when, as mentioned in Section 2, towards evening extremely hazy air was supplanted in unusual manner by considerably less aerosol-containing air although the valley wind persisted. Fig. 2 shows again the temporal trend of the extinction coefficients in the visual (σ_{VIS}) and infrared (σ_{IR}) range. After initial cloud extinction a rather high visible extinction through dry aerosol is measured after 10.00 h with σ_{VIS} values of about 1 km^{-1}. After 16.00 h, the extinction in VIS decreased to about one tenth and just so, with reservation as to the as yet only provisional calibration, in the infrared range. However, it is also possible that the decrease of σ_{VIS} was caused by a reduction of water vapor absorption because parallel with the change to a less hazy atmosphere there occurred a marked drop in humidity from 48 to 38% in the valley, and from 76 to 46% at the Kreuzeck.

The reason for the weak response of IR-transmission to dry aerosol is apparently to be sought in the fact that in this aerosol the concentration of particles contributing to extinction is too small. This concerns particles in the size range above about 10 µm - the aerosol prevailing as a rule in our regions. An above-average high concentration of large particles is found however in Sahara-dust which arrived during our measuring campaign on 2 February 1981. The particle size spectra in this aerosol are essentially smoother, as shown by a comparison between Knollenberg spectra from the Kreuzeck this day (Fig.3) and the spectra from 23 February (Fig.4). However, a marked IR-extinction is not observed in the Sahara aerosol either. According to provisional calibration, σ_{IR} remained on 2 February below 0.05 km^{-1}.

3.2.2. Clouds and fog

From some earlier measurements it is known that extinction in clouds and fog is very high, not only in the visible but also in the infrared channel. That's why still measurable transmission values are only found when the paths within the cloud are not too long, maximally some 100 meters. Within such regions nearly all cloud types are most inhomogeneous. This was confirmed ever and again by the numerous measuring campaigns performed during cloudiness in the reporting period. As a result strongly fluctuating values occur. Within a few seconds the transmissometer reading may vary by orders of magnitude so that it needs sometimes great attention to keep the reading in usable limits through adaption of the gain factor.

The manual evaluation of such strongly fluctuating curves as has been done so far requires a great amount of time and effort. Therefore, a small program was prepared for our desk computer which is equipped with a curve analyzer (digitizer), a plotter, as well as tape reader and tape punch, and a cassette drive mechanism. Through scanning of the measuring curve on the writing tape, transmission factor (in %), extinction coefficient, and time coordinate are entered and punched on tape. This tape

then is input again and the extinction coefficient plotted as a function of time.
The curves shown in Figs. 1 and 2 are direct copies of such plots. This procedure saves already a lot of time compared to the manual evaluation. Due to the limited storage capacity of the desk computer automatic performance of special tasks such as, for instance, establishment of correlations infrared/visual is not yet possible, however. This requires application of a larger computer using the punch tapes provided by the desk computer. The larger computer is available at the Institute but still some programming work is needed.

It was shown in the last interim report by a correlation diagram (Fig.20) that cloud extinction in the infrared range is, as expected, not inconsiderably less than that in the visible range. The diagram in Fig.5 of the present report shows in analogous manner some more recent results where we have differentiated this time by cloud types. Interestingly, it appears that the correlation for stratus runs distinctly steeper as for cumulus clouds, i.e., the ratio infrared/visible extinction is smaller for the former cloud type and amounts to about 1:6.5 compared to 1:2 for cumulus. The cause may surely be sought in the different droplet size distributions in both cloud forms. In the Knollenberg particle size spectra, measured at the station Kreuzeck, the differences between stratus and cumulus are clearly evident. Figs. 6 and 7 show droplet size spectra of stratus and cumulus, respectively. The steeply falling spectra in both diagrams stem from dry aerosol outside the clouds (spectra before 16.00 h in Fig.6, and about 09.00 h in Fig.7). The cumulus spectra in Fig.7 show a deep minimum in the size range from about 2 - 3 µm diameter which does not exist in the stratus spectra (Fig.6). In those we note even in the range from 1 - 2 µm diameter a distinct concentration excess compared to the cumulus spectra. Since particles in this size range contribute to extinction only in the visual range, the different extinction ratios infrared/visible for the two cloud types can be explained in this way.

At this point it should be noted that all extinction coefficients shown so far represent mean values over the entire measuring path. Since in the presence of clouds in the measuring path extinction takes place dominantly in the cloud-filled part of the path which at still measurable transmission is always small compared to the total path, the mean values in these cases are invariably much smaller than the real extinction coefficients within the cloud. In order to establish those, the cloud thickness along the measuring path must be determined. With strongly inhomogeneous clouds this is almost impossible in the majority of cases. On 17 February, however, a nearly stationary stratus sheet extended for a scant hour to closely below the Kreuzeck station. Its base could well be traced by lidar shots in five-minute intervals and the extinction fluctuated just moderately. Fig.8 shows for the whole day the trend of the extinction coefficients and transmission, respectively, which appears for the most part very chaotic. Poorly suited parts of the curves are connected by straight lines which do have no further meaning. Conspicuous is, however, the time period with considerably weaker fluctuations between 17.00 and 18.00 hs. Table 1 gives for this period the cloud thicknesses derived from the lidar data (i.e the length of the measuring path within the clouds), the infrared and, as far as measurable, visual extinction values as well as their quotients σ_{IR} and σ_{VIS}.

The extinction coefficients are averaged over cloud thickness d. An increase of these coefficients with d is recognized in outlines which is well understood as the thickness of the cloud surely grows from its base upwards.

On 25 February it was possible to measure the transmission through a stratus sheet lying fully between valley and Kreuzeck level. From visual observations at the station Wank (1800 m) from above and lidar observations from below its vertical thickness was determined to 170 m which results in a path length of 515 m along the transmission line tilted by 17.25^{o}. From the measured infrared transmission of 0.93% an extinction coefficient of 9.1 km^{-1} is calculated, visible transmission was unmeasurably small, i.e.

σ_{VIS} greater than 20 km^{-1}. These values are essentially higher as the afore-mentioned ones for comparable cloud thicknesses although the cloud type was the same. This, again, indicates that the thickness of the cloud is less at its base than at the top, or on the average.

Table 1: Measured extinction coefficients in stratus, d = cloud thickness measured by lidar along the measuring path. 17.02.1981.

Time (CET)	d (m)	σ_{IR} (km^{-1})	σ_{VIS} (km^{-1}	σ_{IR}/σ_{VIS}
16.53	625	4,04	---	---
17.01	590	3.96	---	---
17.05	545	2,95	---	---
17.10	270	3,64	---	---
17.15	270	3,36	---	---
17.20	290	2,46	12,0	0,205
17.25	290	2.76	15,8	0,175
17.30	280	2,09	13,6	0,154
17.35	250	2,85	16,3	0,175
17.40	290	3,14	15,9	0,198
17.45	290	3,14	16,5	0,190

3.2.3. Extinction at rain

In the preceding Interim Report we described some data obtained during rain which could in part be correlated also with the measured precipitation rates. It was shown above all that, in contrast to dust and clouds, the infrared radiation is more weakened than the visible radiation. This finding is confirmed by more recent measurements. All data obtained since preparation of the 3rd Interim Report are (similarly to Fig.20 of that report) presented in Fig.9 of this report in form of a correlation between visual and infrared extinction including snowfall data. A rather close correlation emerges, exactly in keeping with the one observed earlier (Fig.20, 3rd Interim Report). Here it must be noted that according to Mie-theory which provides reliable results for water droplets, the visible and infrared extinction for raindrops being large compared to the wavelength of visible and infrared radiation, should normally be identical. The lesser apparent extinction for VIS is surely due to the more pronounced forward scattering in this range which may lead to the fact that because of the not infinitely small receiver field-of-view a larger amount of the already deflected light is still concurrently measured. In the literature some methods are described permitting to calculate these effects with the aid of Mie-theory or by approximation methods where the receiver field-of-view and the droplet size distribution enter as parameters. By means of these parameters our transmission data will be corrected in the future. Since the examples calculated in the papers do not apply to our conditions, the correction factors must be re-calculated which requires, however, despite the use of approximation methods quite a lot of effort.

The diagram Fig.10 shows finally the dependence of extinction coefficients on the precipitation rate as far as the latter was measurable. Included in this diagram, too, are the earlier presented data (Fig.19, 3rd Interim Report). We recognize, on the one hand, that rather high extinction coefficients are measured in part at low precipitation rates whereas the values at high

precipitation rates increase just moderately. Here, the delayed response of the rain gauges during beginning precipitation could play a role but also the droplet size distribution entering in a twofold way in the extinction efficiency. First, at given precipitation rate, the sum of the geometrical cross sections of all droplet diameters is inversely proportional to their diameter and, second, the volume concentration of small droplets, again at given precipitation rate, is higher because it is inversely proportional to the velocity of fall which increases with the droplet diamater. Thus, it is understandable that at low precipitation rates which are showing frequently a parallelism with small mean droplet diameters very high extinction values may occur.

If r is the precipitation rate in mm/h, v the fall speed of the droplets, and d their diameter (monodisperse distribution assumed) then results for the extinction coefficient σ_{ext}, which according to Mie-theory for large particles is equal to the double geometrical cross section, the relationship

$$\sigma_{ext} = \frac{5}{6} \cdot \frac{r}{vd} \quad .$$

Since v increases at least proportional to d, a rather steep increase of σ_{ext} with decreasing droplet diameters will result.

3.2.4. Extinction at snowfall

Diagrams 9 and 10 include also the extinction data found so far. The ratio of visible to infrared extinction coefficients (Fig.9) is about the same as during rain. For establishing a correlation between transmission during snowfall and precipitation rate the available material is not yet sufficient. The snowfall rates remain mostly below the response level of the measuring instruments. The few rare existing data are entered in diagram 10 as triangle symbols. It looks as if during snowfall the extinction at given precipitation rates is considerably higher than during rain, as

it was to be assumed, and that during well measurable snowfall rates the transmission nears quickly the lower detection limit.

4. Some Remarks on the Evaluation of Lidar Signals

The computer program set up several years ago at the Institute for deriving the aerosol concentration and size distribution which has been extensively described in previous relevant reports proved very time-consuming and moreover instable against errors in both the measured values themselves and the entering additional parameters such as refractive index and scattering property of particles, calibration factors, etc. Often the lidar profiles and just so the additional parameters have to be modified in order to reach a physically meaningful result altogether. Thus, the method is poorly suited for arriving quickly and without problems at results - if possible even through the computer itself which is installed in the lidar. Such instabilities are, as follows from the relevant literature, inherent to most methods for solving the lidar equation. Recently, J.D. Klett (1981) suggested an approach avoiding such instabilities. The method proceeds from the fact that the lidar equation has an analytical solution assuming that there exists between backscatter coefficient β and extinction coefficient σ an exponential relationship of the form $\beta = \text{const} \cdot \sigma^k$ where the value of the constant must not be known. This relationship can be regarded as approximately valid whenever molecular scattering can be neglected, i.e., at low visibilities or when the lidar wavelength is in the near-infrared. Hence, under these conditions one obtains an analytical expression as solution of the lidar equation which indicates the extinction coefficient as a function of distance. It contains as integration constant the extinction in a certain reference distance, further parameters do not enter. Klett has shown that the solution is stable against measuring errors such as noise etc., and just so against the choice of the integration constants if one chooses only the end and not the beginning of the measuring path as reference distance. The method is further of advantage inasmuch as it does not require calibration of the lidar.

We will try in the future to apply this method for our lidar measurements between Institute and Kreuzeck station at low visibility conditions. Klett's expression is relatively simple, a provisional program for its calculation was already developed and can easily be accommodated in the recently extended core memory of the computer in the mobile lidar. As reference unit we choose conveniently the distance to the Kreuzeck since measured aerosol data are here available. Possibly, even visibility data may suffice.

Furthermore it is attempted at present to derive from the lidar profiles between Institute and Kreuzeck (since starting of operation at the station Kreuzeck more than 1000 individual profiles have been obtained) an empirical relationship between lidar backscatter and extinction on the one hand, and the measured aerosol data on the other, which might be a valuable supplement to the Mie-theory.

(Dr. R. Reiter)
Director
Principal Investigator

Reference

J.D. Klett: Stable analytical inversion solution for processing lidar returns. Appl. Opt. 20, 211 (1981)

ANNEX

FIGURES 1 - 10

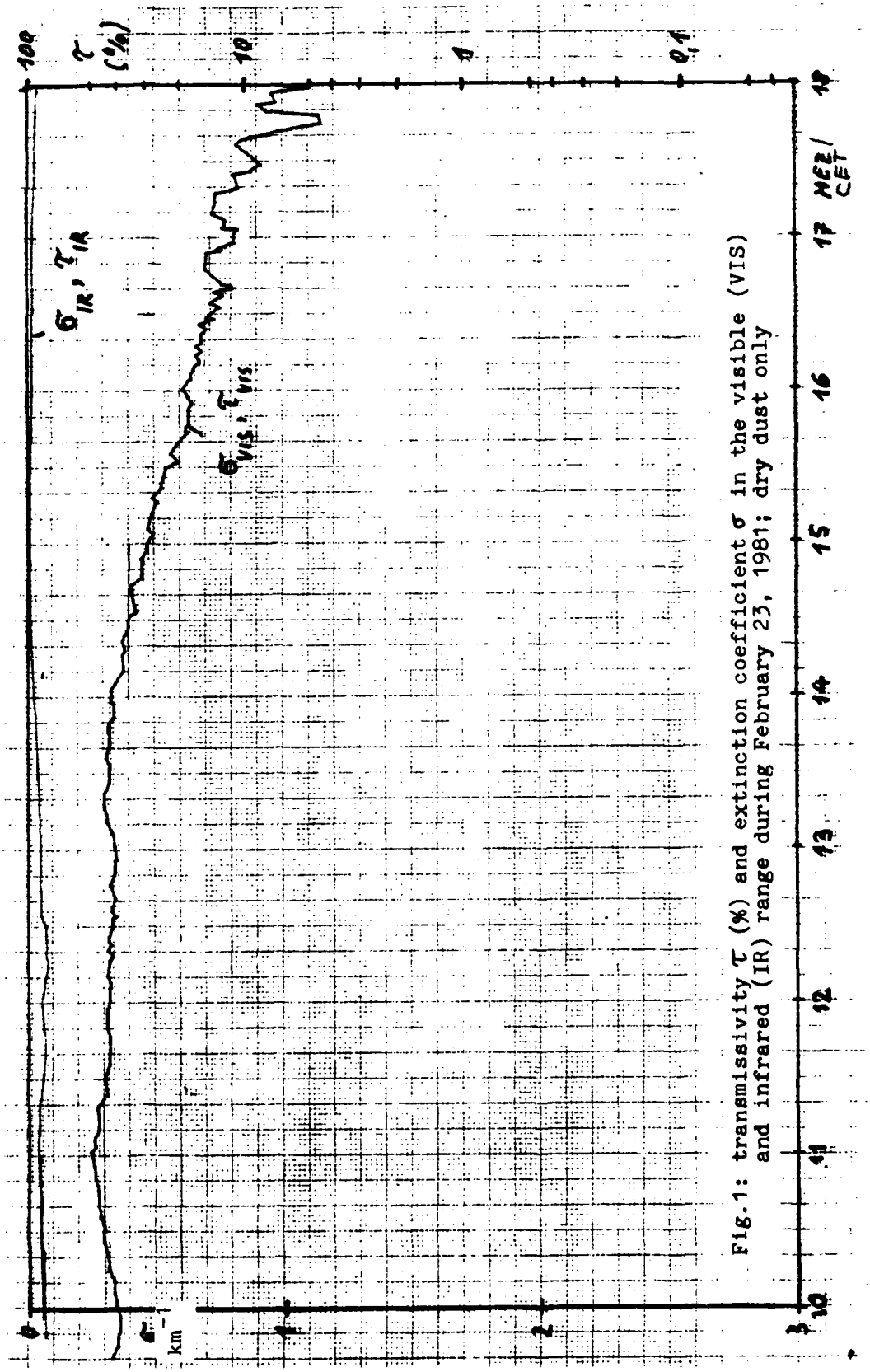

Fig.1: transmissivity τ (%) and extinction coefficient σ in the visible (VIS) and infrared (IR) range during February 23, 1981; dry dust only

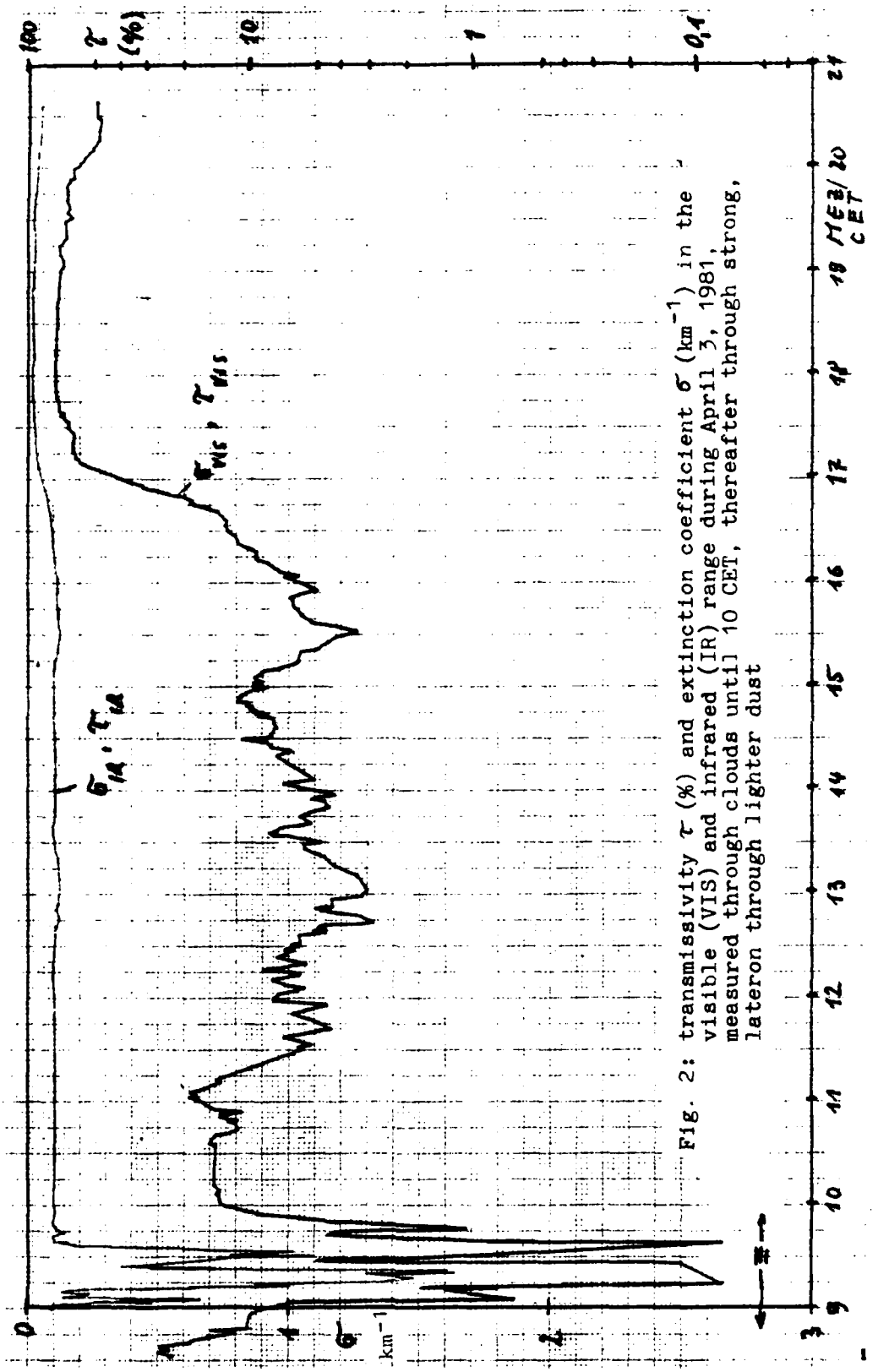

Fig. 2: transmissivity τ (%) and extinction coefficient σ (km^{-1}) in the visible (VIS) and infrared (IR) range during April 3, 1981, measured through clouds until 10 CET, thereafter through strong, lateron through lighter dust

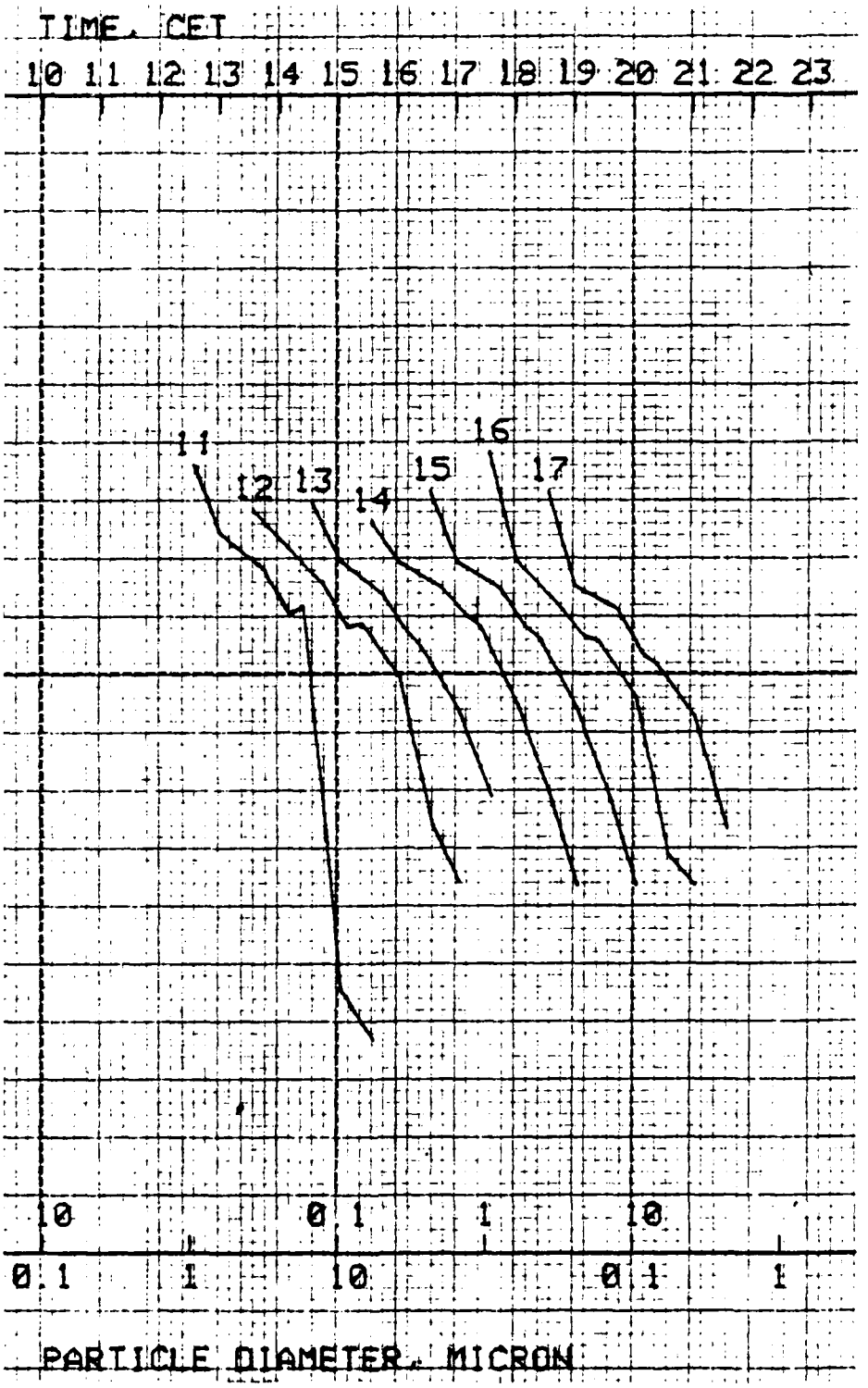

Fig. 3: size distributions of dust particles from the Saharan desert, measured on Feb. 2, 1981, by Knollenberg spectrometer at the Kreuzeck station

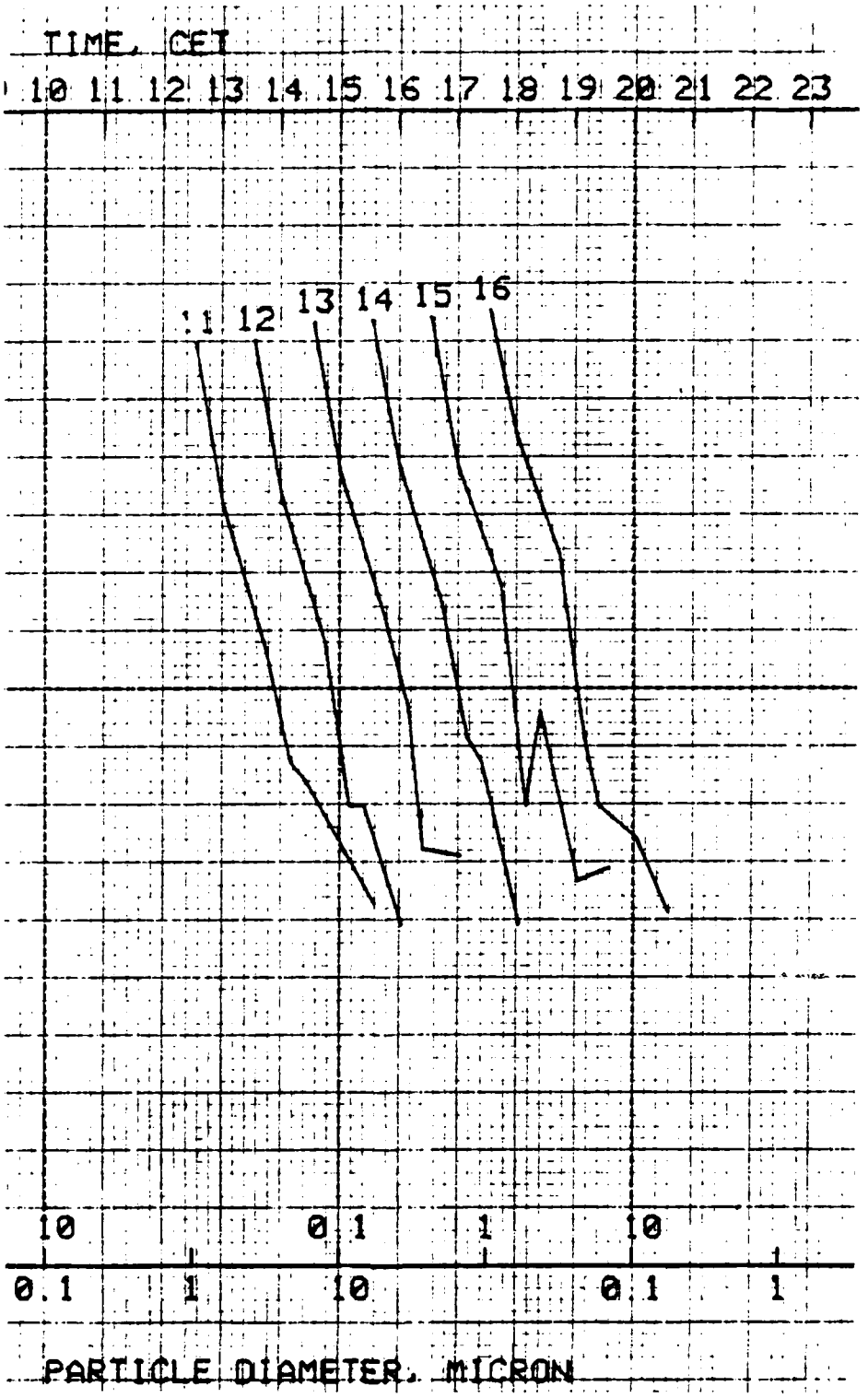

Fig. 4: size distributions of typical aerosol particles from the vicinity of Garmisch-Partenkirchen, measured on Feb. 25, 1981, by Knollenberg spectrometer at the Kreuzeck station

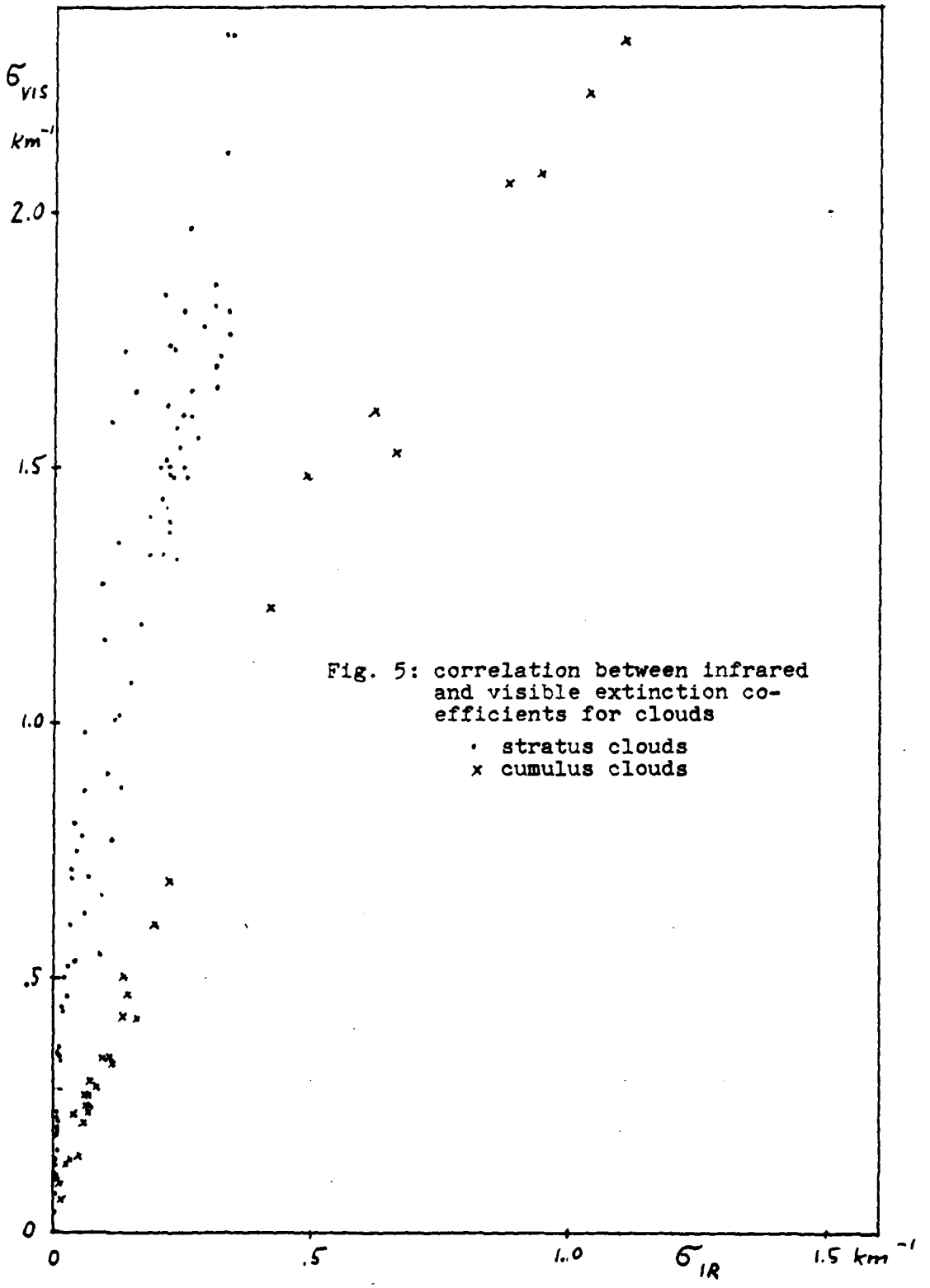

Fig. 5: correlation between infrared and visible extinction coefficients for clouds

• stratus clouds
x cumulus clouds

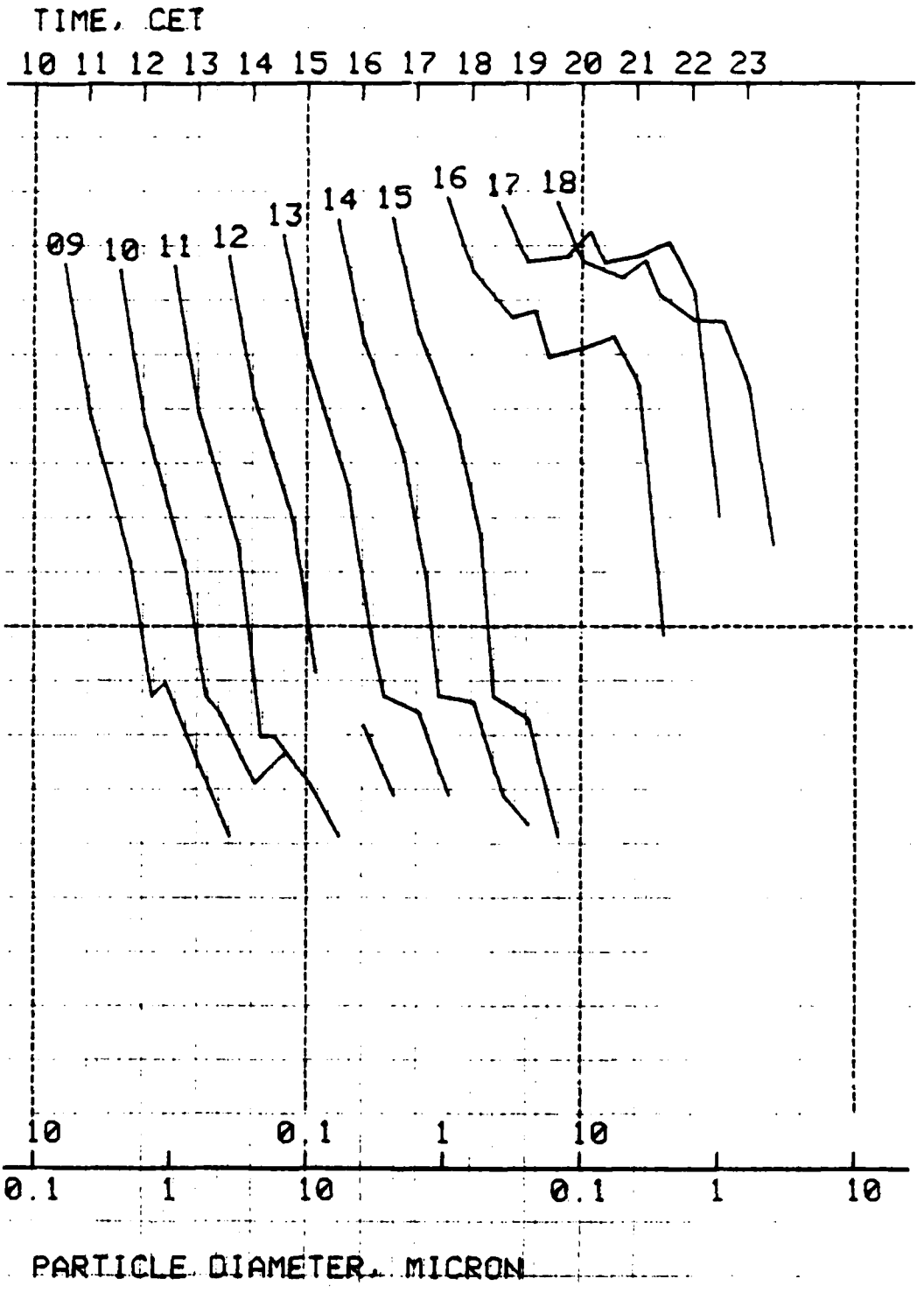

Fig. 6: particle size distribution within stratus, measured on Feb. 17, 1981, at the Kreuzeck station

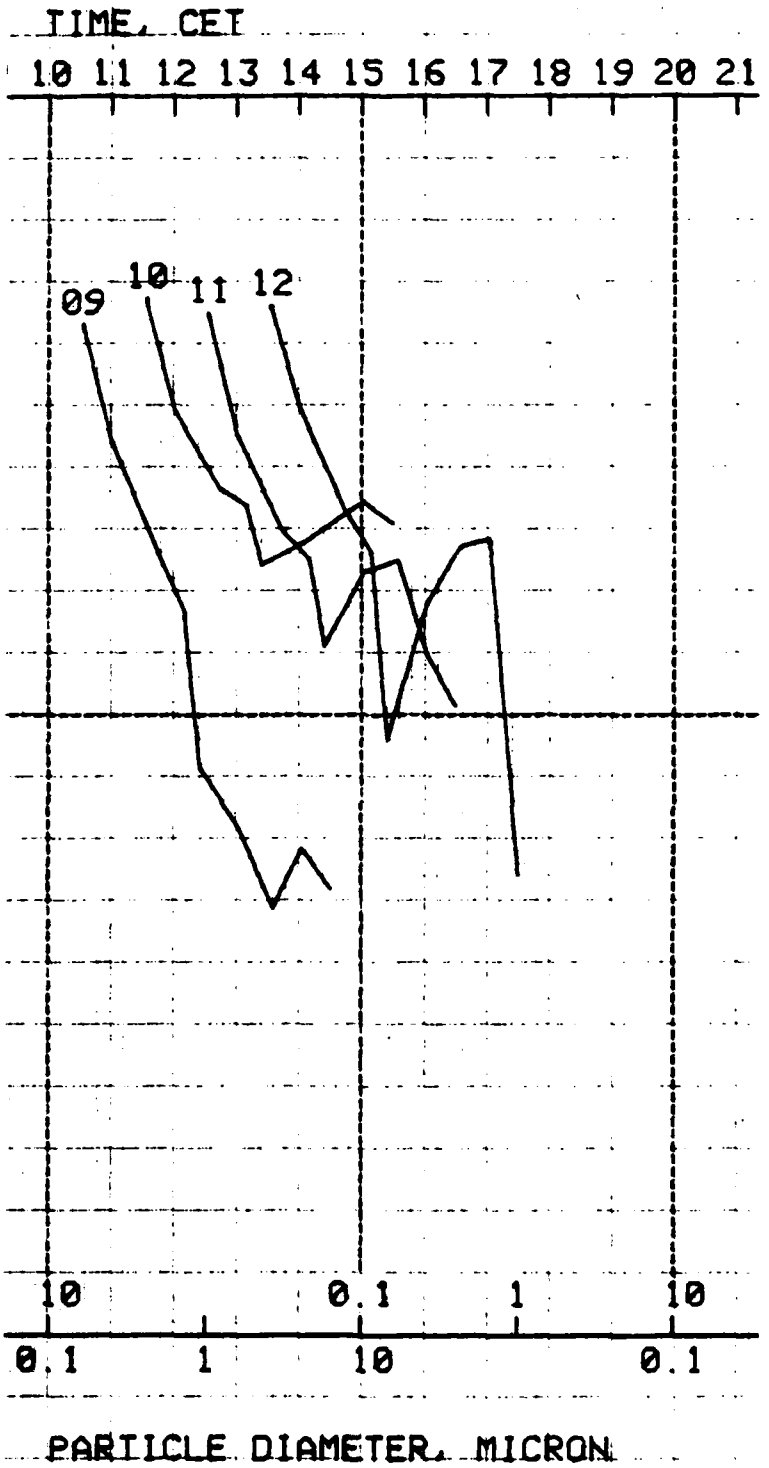

Fig. 7: particle size distribution within cumulus, measured on April 6, 1981, at the Kreuzeck station

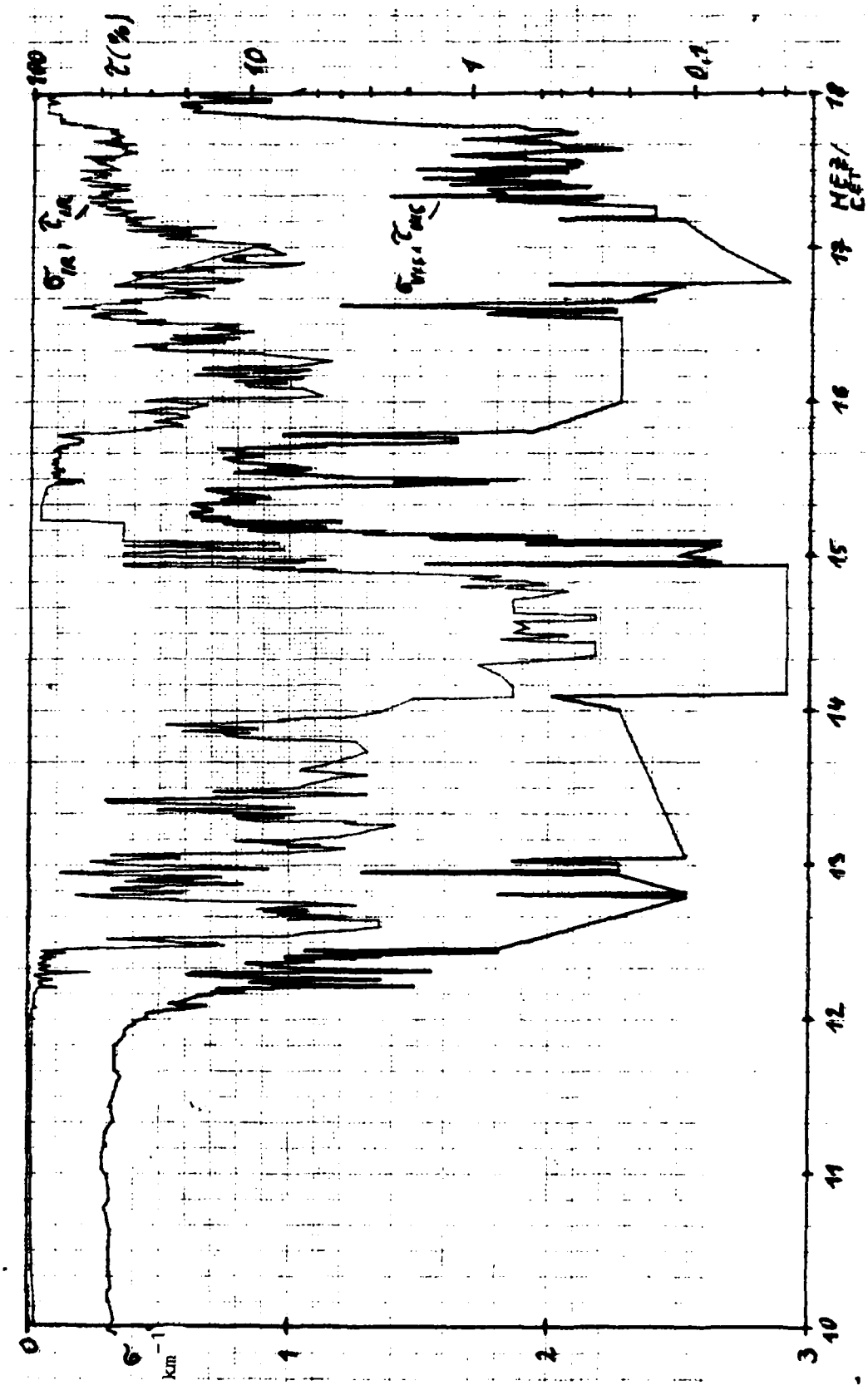

Fig. 8: transmissivity τ and extinction coefficient σ in the visible (VIS) and infrared (IR) range on February 17, 1981, with stratus clouds being temporarily present within the transmission path

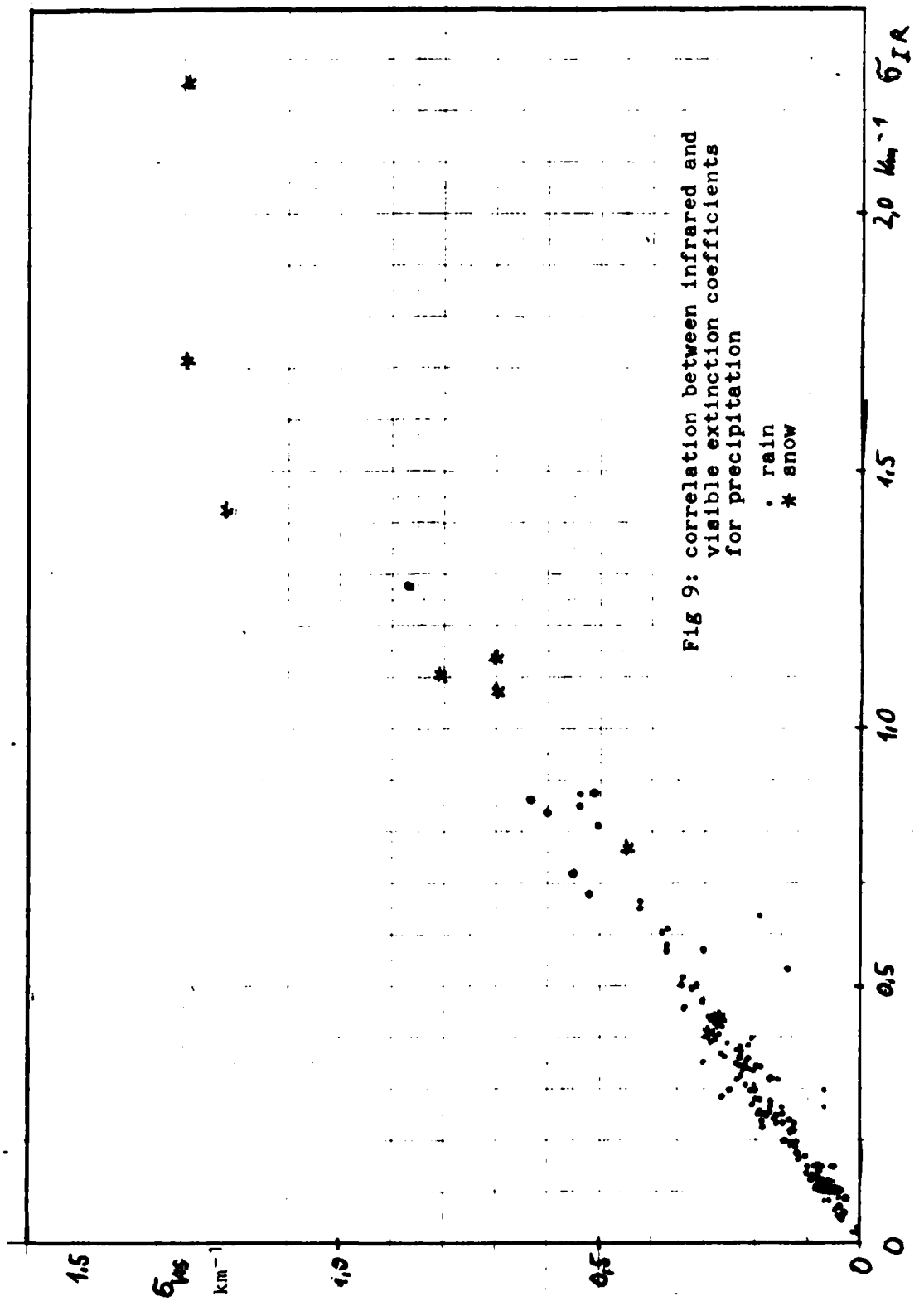

Fig 9: correlation between infrared and visible extinction coefficients for precipitation

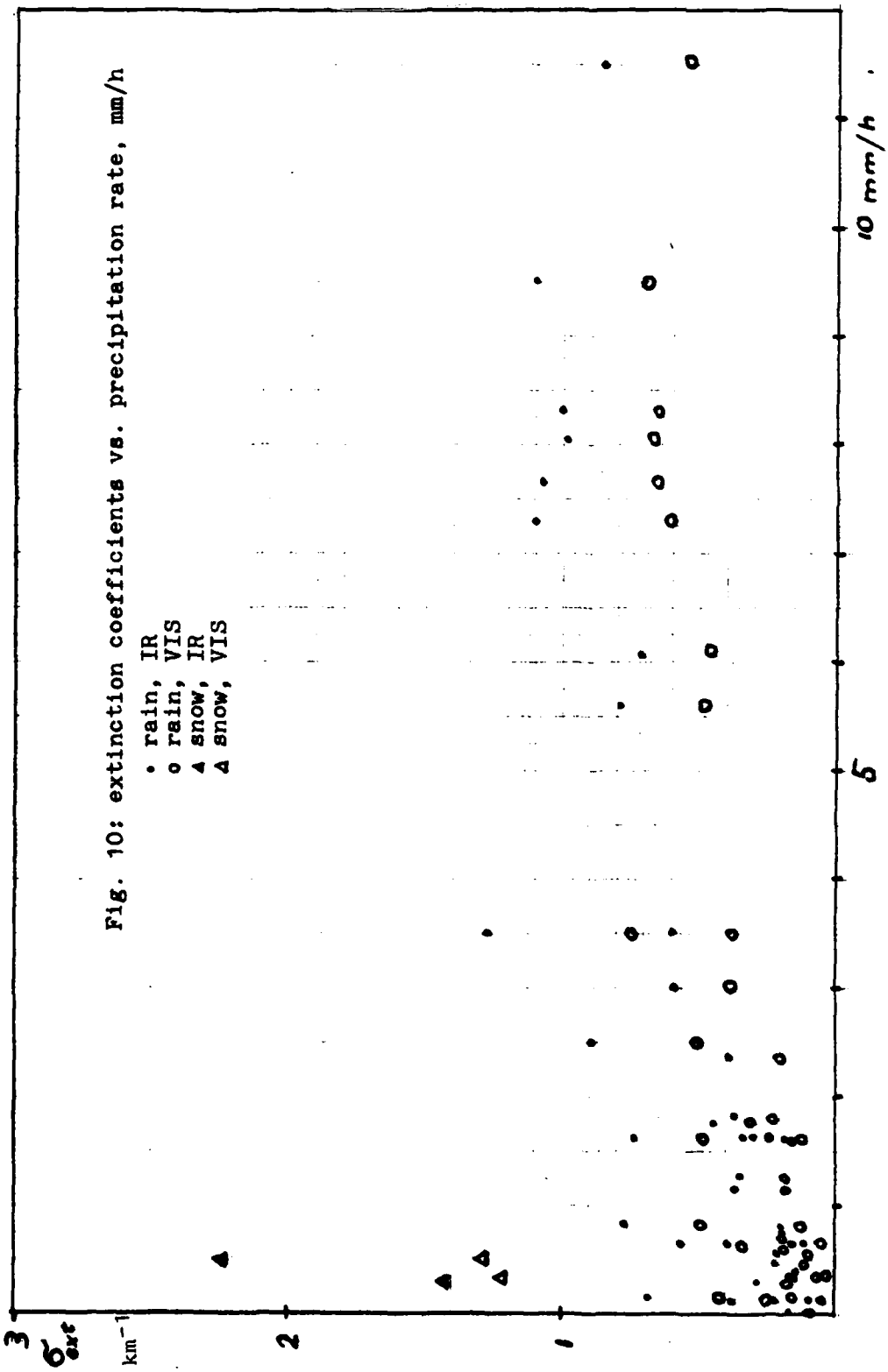

Fig. 10: extinction coefficients vs. precipitation rate, mm/h
• rain, IR
o rain, VIS
▲ snow, IR
△ snow, VIS

A P P E N D I X

Supplement for the period 1 August through 31 December 1981

(all figure numbers and table numbers given in the following apply to this APPENDIX, except a page number is added)

1. Recent Developments in the Technical State of the Measuring Systems

No serious problems arose during the last half year with the Barnes transmissometers. Meanwhile ten spare halogen lamps for the visible light source are available, and a calibration device is ready for operation, which allows measurement of the relative lamp brightness close to the receiver after suitable attenuation by neutral density filters. So in the future the replacement of the lamps will no longer be a time-consuming procedure. The infrared transmissometer was suspected during the last year to be somewhat instable. As any misalignments or dirt deposits on optical parts could be excluded as reason for this instability, the blackbody temperature shall be measured in the future by means of a thermocouple and transmitted to the institute via the existing telemetry line. In the meantime, however, it was found that the apparent instabilities of the infrared transmissometer readout under clear atmospheric conditions were simulated by variations in the water vapor absorption, as will be discussed later. So at least during the last year that transmissometer seems to have been stable.

In the mobile lidar system, the development of a signal detector and energy monitor for the fourth wavelength, 1060 nanometers, is completed. Since the initial plan to cover the total wavelength range from 347 to 1060 nm by a single semiconductor detector could not be realized (the initially envisaged UV-photodiode is sufficiently sensitive but not fast enough in the infrared), we must use both the S-20 photomultiplier tube and an infrared photodiode detector. A mechanical device for a quick interchange of both detectors has been constructed.

2. Compilation of Transmissometer Measurements Since August 1981

2.1. 07 August 1981, 11.00 - 13.44 CET

This day a front with altostratus and altocumulus clouds was approaching from the west, and rainfall was expected. However, only around noon some precipitation occurred, which remained below the detection threshold of the rain gauges. In the afternoon the weather grew better rapidly, and the measurement was finished.

2.2. 01 September 1981, 07.00 - 10.50 CET

In connection with a cold front passage rain showers occurred repeatedly. Due to simultaneously occurring clouds within the transmission path almost no usable data were obtained, however. In the course of the forenoon the path became completely blocked by clouds and the measurement was stopped.

2.3. 03 September 1981, 07.00 - 16.48 CET

At the border of a high over the North Sea cold air was flowing from northern to north-eastern directions across Central Europe. In the early morning a stratus cover was observed above 1150 to 1250 m ASL, showing some dissolution tendencies. Underneath it was quite hazy, the visual range was 4 km. At 3400 m ASL (altitude determined by lidar) altostratus was found. The lower stratus was almost completely dissolved when the blackbody had reached its nominal temperature, so that only very few usable transmission data were obtained.

2.4. 08 September 1981, 04.00 - 18.00 CET

The campaign was carried out in connection with a mountain-valley breeze measuring experiment. At the end of a high-pressure period fairly warm air was flowing in from SW (air mass type xS_p), in which a visual range of 20 to 30 km was measured. In the afternoon high-level clouds indicated the approach of a rain front. At 6 PM the measurement was stopped because of beginning rain. In the visible as well as in the infrared wavelength range the transmission decreased in the course of the day, in the latter case because of increasing water vapor concentration, as will be shown later on.

2.5. 12 October 1981, 08.40 - 17.35 CET

In a strong north-westerly upper flow a small secondary cyclone was approaching this day, accompanied by increasing altostratus clouds and slowly descending virga, where maritime polar air (mP) was temporarily replaced by maritime subtropical air (mS). At 10 AM rainfall began also in the valley. During the measuring period 7 mm precipitation were recorded in the valley, but only 3.9 mm at the Kreuzeck station. It is well known that on mountain peaks during strong winds often too less precipitation is measured, but in this case the Kreuzeck value should be real, because the mean wind speed at that station was around 1 m/s. Furthermore, the cloud cover above the Kreuzeck station looked always lighter than in the zenith. Since, as usual during rainfall, small cumulus fractus clouds were drifting through the transmission path, continuous observation of the path and recording of the cloud-free intervals was strictly necessary in order to obtain usable precipitation extinction data.

2.6. 15 October 1981, 08.00 - 17.20 CET

Also this day a low surpassed southern Central Europe within a zonally directed frontal zone and the preceding warm front was accompanied by temporarily strong rainfall from nimbo-stratus clouds. The total amount of rainfall was 4 mm in the valley and 2.4 mm at the Kreuzeck, where the mean wind speed was again below 1 m/s. Intervals with cloud-free transmission path were again found out by continuous eye observation.

2.7. 30 October 1981, 08.00 - 17.30 CET

As very frequently during this October, the weather situation was again determined by the influx of maritime air (mS_p and mP_S) from the west. In the morning the approach of stratiform clouds was observed, and at 8 AM rainfall began, mostly with low intensity. Again the temporary occurrence of clouds in the transmission path required its continuous observation. The measured amount of precipitation was 3.2 mm in the valley, and 1.7 mm at the Kreuzeck. The wind speed data from the Kreuzeck (average 1.1. m/s, maximum 4 m/s) make the rainfall values again look real.

2.8. 03 November 1981, 07.35 - 11.14 CET

An anticyclone over southern Central Europe and warm, sub-tropical air (xS) determined the weather this day. In the morning a thin stratus layer was present above the institute site, with a lower boundary at 850 m ASL (120 m above ground level), showing dissolution tendencies in the west. Until 9 AM this layer had dissolved except for some remaining small clouds at the mountain slopes, and the visibility was increasingly good. Later on, towards noon, a foehn-like cloud pattern with rapidly changing cumuli and altocumuli was observed, causing an extremely high background brightness in the direction of the transmission path due to the low elevation of the sun.

In order to avoid any damage of the transmissometers the measurement was stopped.

2.9. 04 November 1981, 07.00 - 22.00 CET

This extended campaign was again started together with another mountain-valley breeze experiment. Under the influence of a weakening high over Middle Europe cloudless fair weather was prevailing, and within a subtropical air mass (xS) very good visibility was observed. In the valley the visual range was more than 40 km before noon, at 1800 m ASL more than 100 km. Consequently, no aerosol backscatter is found in the lidar returns. Not before the onset of the valley breeze at 13.30 CET, which was not very strong in this case, some aerosol was flowing in, reducing the visual range to about 23 km. In the lidar profiles a weak upper dust boundary at 1000 m ASL could be identified which ascended rapidly with time and became more pronounced. At 4 PM it was found at the Kreuzeck station level (1630 m). Above this ground layer the aerosol increased too, probably indicating the approach of a cold front from NW. The recorded increase of the humidity at 1630 m as well as the decreasing visibility at 1800 m ASL might have the same reason. Towards the end of the measuring period at 22 CET the vertical lidar shows an already quite pronounced dust layer from the ground up to 2900 m ASL, while in 5500 m first indications of approaching clouds are found.

3. Results to Date

In this chapter a summarizing presentation of the results gained during the last year will be given. Some of the diagrams obtained until July 1981 which are presented on pages 19 - 28 have been updated and will be shown in this appendix

again in extended form. Like in the previous reports the results are grouped according to the three main types of light extinguishing media, namely dry aerosol, clouds and fog, and precipitation.

3.1. Dry Aerosol

Our previous experience that dry aerosol in the absence of clouds and precipitation affects the transmission significantly only in the visible region, has been further confirmed by the recent measurements. The IR transmissometer readout shows under dry aerosol conditions variations from day to day which are obviously, if at all, only very weakly correlated to the aerosol concentration. So it was suspected that the IR transmissometer is somewhat instable. Another reason for those inconstancies of the IR level could be concentration variations of IR absorbing gaseous atmospheric constituents, mainly of water vapor (absolute humidity). As already mentioned earlier, the LOWTRAN code, which is required for the calculation of the molecular absorption, cannot be run on our computer. By the beginning of February 1982, however, a new, much larger computer system with 512 k Bytes memory and 320 ns cycle time will be available. A powerful system software allows multi-user operation with 768 k Bytes virtual memory peruser. On a machine of this type a test run of the LOWTRAN 5 program has been carried out sucessfully with a CPU time of 25 seconds. In the meantime it was tried to find an empirical relation between absolute humidity and IR amplitude. For this purpose at first absolute humidities were calculated from the meteorological data from the Institute and the Kreuzeck station. The mean values from both stations were correlated to the logarithms of the IR amplitudes (Y_{IR}). Fig.1 shows the result. Despite some scatter of the data points a rather close correlation shows up. The diagram includes also the calculated regression line. It is to be emphasized, however, that a linear regression between

absolute humidity a and log Y_{IR} implies the validity of BEER's extinction law which is fulfilled approximately at most in this case. The scatter of the data points may have several reasons. For example, other parameters could contribute to the IR extinction (aerosol!), or the mean value of the absolute humidities at the Institute and the Kreuzeck may not represent the average water vapor concentration along the transmission path correctly. Exact average absolute humidities were calculated, therefore, from our radiosonde data and similarly correlated to log Y_{IR}. Fig.2 shows this correlation, which is significantly closer than that in Fig.1. The regression line, which is about the same as in Fig.1, describes a proportionality between a formal water vapor absorption coefficient σ_a in km^{-1} and the absolute humidity a in g/m^3:

$$\sigma_a = .0188 \cdot a \qquad (1)$$

This finding results in some important consequences. First, the influence of water vapor on the IR transmission is quite remarkable, at medium absolute humidities the transmisssion is already reduced by about 15%. The quite close correlations Figs. 1 and 2 show that our suspicion of an instability of the IR transmissometer is not justified at least for the past year. The hitherto only provisional 100%-values for IR may now be replaced by a much higher one, which should be already a good approximation of the true value. We can look forward with great interest to a comparison of the empirical relation (1) with the results of the future LOWTRAN calculations.

The new IR reference value was used to calculate all transmissivities for dry aerosol conditions from the data after October 1980. The results are shown in Tables 1 - 8, together with the data for the visible range and with temperatures and relative and absolute humidities at the Institute (G) and the Kreuzeck station (K), and the visual ranges V at the Institute and for the Wank peak station (W) at 1800 m ASL. The visibility

meter for the Kreuzeck station was not yet installed there.

Finally the water vapor turns out to be the predominant parameter for the IR extinction, especially with respect to the aerosol. To demonstrate this, in Fig.3 the IR extinction coefficients, σ_{IR}, are correlated to those for the visible, σ_{VIS}, for dry aerosol conditions (i.e. the data from Tables 1 - 8). It is to be seen that no or at least very poor correlation exists (σ_{VIS} is under dry conditions only affected by the aerosol). As a last step, the σ_{IR} data were corrected for H_2O absorption and again correlated to the σ_{VIS} data (Fig.4). The absence of a correlation is even more obvious in this diagram. The lone exception are the data from April 3, 1981 which are shown off by another point symbol. As described in detail on page 9 of this report, this day a remarkable decrease of both aerosol concentration and humidity occurred, accompanied by a significant increase of the IR transmission. The σ_{IR} data from this day show a close correlation to σ_{VIS} still after the water vapor correction. The reality of this result must be proved by future LOWTRAN calculations.

3.2. Clouds and Fog

In contrary to dry aerosol, transmission through clouds and fog is always subject to heavy fluctuations, which make a tabular presentation of the data difficult. So we still prefer in this report the more clear form of correlation diagrams. Fig. 5 on page 23 illustrates the relation between visible and infrared extinction coefficients for clouds. The data are averages over the total transmission path lengths, and since clouds with still measurable transmissivity always fill only a small part of the path,those averages are much smaller than the true cloud extinction. Similarly, the variation range of the data does not represent actual variations of the true extinction coefficients, but rather variations of the cloud

thickness along the transmission path. This does not affect, however, the correlation behavior of the data. The extinction coefficients were grouped with respect to cloud types, and we found that the ratioes $\sigma_{IR}:\sigma_{VIS}$ for cumulus clouds differ from those for stratiform clouds, which could be explained by the differing droplet size distributions as measured by the Knollenberg spectrometer. In Fig.5 of this appendix the correlation has been updated by including new data. We see some new stratus data, which do not agree with the former ones. Furthermore, a series of extinction coefficients of thin, rapidly changing cumulus fractus clouds showed a considerable scatter in the $\sigma_{IR}:\sigma_{VIS}$ ratio and could not be included in one of the former two data groups (cumulus and stratus clouds). Some of them are found between the cumulus and stratus branches, the majority, however, still beyond the latter branch. Such short-lived clouds exist apparently of much smaller droplets than the already "aged" stationary cumulus mediocris, from which the data in the cumulus branch are resulting.

As mentioned above, the derivation of true cloud extinction coefficients requires the knowledge of the cloud thickness along the transmission path which is often difficult to measure. In some favorable cases, however, we are able to do this. A number of data has already been presented in Table 1 on page 13. In the meantime two more such measurements could be carried out. The results are included in the updated Table 9.

3.3. Extinction by Precipitation

Due to the unusual high frequency of precipitation during the past half year a series of good data for transmission through rain were obtained during that period. It was confirmed that during precipitation the transmission in the

infrared is always less than in the visible. Fig.6 shows the updated correlation diagram where in contrary to the corresponding diagram Fig.9, page 27, a logarithmic representation was chosen in order to avoid overloading of the figure with data points in the lower range. The regression line in the former linear diagram corresponds to a proportionality between σ_{IR} and σ_{VIS}. In the logarithmic diagram a proportionality is a straight line tilted under 45 deg., but with a deviation from the origin. The points in Fig.6 turn out to be oriented along such a line at least in the upper part. The regression line describes the proportionality

$$\sigma_{VIS} = .64\ \sigma_{IR} \qquad (2)$$

In the range of smaller values increasing deviations of the points from the regression line are observed which are at least in part surely real.

It has already been pointed out earlier that according to the Mie-theory the extinction coefficients for spherical particles such as rain drops should be equal for the IR and visible region. In the previous sections it was presumed that the apparently smaller extinction in the visible is caused by the more pronounced forward scattering in this range. Due to the not infinitely small field of view (FOV) of the transmissometers part of the already deflected light may still enter the receiver and be measured. A. DEEPAK and M.A. BOX calculated the influence of forward scattering on optical extinction measurements for a number of mono- and polydispersed aerosols [Applied Optics 17 (1978) 2900 and 3169]. Accordingly, for water droplets with 1 mm diameter and the FOV of the Barnes transmissometers almost exactly our measured extinction ratio of .64 (2) should result. The measured extinction coefficient in the IR is then 95%, that in the visible, however, only 60% of the true value.

The diagram Fig.7 shows the extinction coefficient as function of the precipitation rate r (mm per hour) for rain and snow. In contrary to the corresponding diagram in Fig. 10, page 28 in this report, only the infrared data are included. The figure contains all data obtained since the beginning of our transmission measurements. It is to be seen that the extinction increases at first rather fast, then more slowly with the precipitation rate. The reason may be a variation of the mean droplet size with r, as already discussed in detail on pp. 14/15.

The scatter of the extinction data is in part surely caused by droplet size variations, in part however, by the delayed response of the rain gauges during beginning precipitation. For this reason we present in Fig.8 the extinction data from two single precipitation events, which were not much affected by that delayed response. As a matter of fact, the scatter of the data seems to be smaller in these two cases, and the dependence of the extinction coefficient on the precipitation rate to come out more clearly.

The diagram Fig.8 contains some data for snowfall obtained during the winter 1980/81 which have already been discussed previously. No further data are available up to now.

TABLES

No. 1 - 9

Legends for Tables 1 - 8

τ_{IR}, τ_{VIS} = transmissivity in % in the infrared and visible range

σ_{IR}, σ_{VIS} = extinction coefficient in km^{-1} in both ranges ($\sigma = (-\ln.01\tau)/2.7$ km)

τ = atmospheric temperature in centigrades

RH = relative humidity in %

a = absolute humidity in g per m^3

V = visual range in km

G = institute in the valley (Garmisch-Partenkirchen), 740 m ASL

K = Kreuzeck station (with radiation source), 1630 m ASL

W = Wank peak station, 1780 m ASL

Table 1: Transmission and meteorological data from 02 February , 1981

Time	τ_{IR}	σ_{IR}	τ_{VIS}	σ_{VIS}	t (^{o}C)		RH (%)		a(g/m^{3})		V (km)	
CET	%	km^{-1}	%	km^{-1}	G	K	G	K	G	K	G	W
10.30-11.30	80.3	.0810	53.1	.234	+ 0.8	+ 5.4	92	24	4.7	1.7	28	54
11.30-12.30	83.1	.0685	54.5	.225	+ 3.2	+ 3.7	81	27	4.9	1.7	29	51
12.30-13.30	85.0	.0605	53.8	.229	+ 5.0	+ 3.7	70	27	4.7	1.7	31	55
13.30-14.30	86.3	.0545	52.8	.236	+ 5.8	+ 2.8	64	29	4.6	1.7	30	61
14.30-15.30	86.4	.0540	52.5	.239	+ 3.4	+ 2.7	66	32	4.0	1.8	28	59
15.30-16.30	81.8	.0745	53.2	.233	+ 1.2	+ 2.4	74	32	3.9	1.8	26	57

Table 2: **Transmission and meteorological data from** 23 February, 1981

Time	τ_{IR}	σ_{IR}	τ_{VIS}	σ_{VIS}	t (^{o}C)		RH (%)		a(g/m^{3})		V (km)	
CET	%	km^{-1}	%	km^{-1}	G	K	G	K	G	K	G	W
09.30-10.30	80.9	.0783	41.4	.327	- 5.8	- 2.0	100	44	3.0	1.8	5.7	24
10.30-11.30	82.6	.0706	48.1	.271	- 4.0	- 3.2	91	44	3.2	1.7	6.4	23
11.30-12.30	85.4	.0587	42.7	.315	- 3.0	- 4.0	87	43	3.3	1.5	5.8	21
12.30-13.30	82.0	.0783	42.1	.320	- 2.9	- 3.9	84	46	3.2	1.6	5.9	18
13.30-14.30	86.2	.0551	39.7	.342	- 2.3	- 3.4	84	48	3.4	1.8	5.9	21
14.30-15.30	89.5	.0412	28.9	.460	- 1.7	- 4.2	81	51	3.4	1.8	5.6	21
15.30-16.30	87.8	.0481	18.0	.635	- 2.0	- 5.2	82	60	3.4	1.9	5.0	18
16.30-17.30	86.0	.0557	13.0	.757	- 2.5	- 5.6	83	59	3.3	1.8	4.5	15

Table 3: Transmission and meteorological data from 03 April, 1981

Time	τ_{IR}	σ_{IR}	τ_{VIS}	σ_{VIS}	t (^{o}C)		RH (%)		a(g/m^{3})		V (km)	
CET	%	km^{-1}	%	km^{-1}	G	K	G	K	G	K	G	W
10.30-11.30	69.6	.132	12.5	.770	+13.3	+9.5	74	55	8.5	5.0	4.9	10.5
11.30-12.30	70.5	.129	6.3	1.024	+14.4	+8.9	73	58	9.0	5.1	4.2	10.7
12.30-13.30	68.6	.139	3.8	1.207	+14.4	+8.8	69	63	8.5	5.5	3.9	6.3
13.30-14.30	70.5	.129	6.2	1.030	+15.1	+8.7	69	55	8.9	4.7	4.0	6.9
14.30-15.30	69.2	.136	7.7	.951	+15.3	+8.0	67	67	8.8	5.6	4.2	7.7
15.30-16.30	68.8	.138	6.2	1.031	+15.0	+6.5	65	76	8.4	5.7	5.2	7.7
16.30-17.30	78.5	.089	33.6	.404	+14.8	+5.3	53	67	6.7	4.7	10.0	7.5
17.30-18.30	87.5	.049	73.3	.115	+14.0	+5.3	41	48	5.0	3.4	18.2	5.4
18.30-19.30	85.9	.056	70.4	.130	+11.9	+5.5	45	55	4.7	3.8	17.2	3.7
19.30-20.30	83.3	.067	57.3	.206	+ 9.0	+5.6	59	61	5.2	4.3	14.6	3.6

Table 4: Transmission and meteorological data from 21 April , 1981

Time	τ_{IR}	σ_{IR}	τ_{VIS}	σ_{VIS}	t (^{o}C)		RH (%)		a(g/m^3)		V (km)	
CET	%	km^{-1}	%	km^{-1}	G	K	G	K	G	K	G	W
09.30-10.30	86.3	.054	62.0	.177	+ 6.2	-0.6	56	66	4.1	3.1	16.1	6.4
10.30-11.30	87.0	.051	70.4	.130	+ 7.3	-0.3	47	64	3.7	3.0	18.6	8.8
11.30-12.30	87.3	.071	70.4	.130	+ 8.9	+0.6	43	58	3.7	2.9	20.8	11.3
12.30-13.30	85.9	.077	73.9	.112	+ 9.6	+0.2	39	55	3.6	2.7	20.5	14.1
13.30-14.30	85.1	.080	72.3	.120	+ 9.6	+0.5	38	56	3.5	2.8	19.0	14.1
14.30-15.30	87.0	.051	74.9	.107	+10.5	+1.4	35	52	3.4	2.8	19.7	14.1
15.30-16.30	86.3	.054	73.7	.113	+10.6	+1.0	32	50	3.1	2.6	18.6	14.6

Table 5: Transmission and meteorological data from 23 April, 1981

Time	τ_{IR}	σ_{IR}	τ_{VIS}	σ_{VIS}	t (^{o}C)		RH (%)		a(g/m^{3})		V (km)	
CET	%	km^{-1}	%	km^{-1}	G	K	G	K	G	K	G	W
09.30-10.30	84.1	.0630	47.6	.275	+ 4.3	+ 0.3	62	54	4.1	2.7	12.4	6.6
10.30-11.30	83.5	.0670	47.3	.277	+ 5.8	+ 0.6	57	55	4.1	2.8	11.9	7.1
11.30-12.30	83.7	.0659	45.5	.292	+ 6.7	+ 0.2	55	59	4.2	2.9	11.2	7.9
12.30-13.30	83.5	.0670	50.5	.253	+ 7.4	+ 0.4	51	59	4.1	2.9	12.3	8.4
13.30-14.30	83.3	.0678	52.3	.240	+ 7.8	+ 0.3	51	59	4.2	2.9	12.6	7.8
14.30-15.30	83.2	.0682	53.7	.230	+ 8.5	+ 0.6	49	59	4.2	3.0	13.0	7.3
15.30-16.30	82.8	.0697	53.2	.234	+ 8.5	- 0.1	50	63	4.2	3.1	12.2	6.5

Table 6: Transmission and meteorological data from 1/2 July, 1981

Time	τ_{IR}	σ_{IR}	τ_{VIS}	σ_{VIS}	t (^{o}C)		RH (%)		a(g/m^3)		V (km)	
CET	%	km^{-1}	%	km^{-1}	G	K	G	K	G	K	G	W
09.30-10.30	55.3	.111	64.7	.161	+13.7	+10.9	64	52	7.6	5.2	21.5	29.3
10.30-11.30	73.5	.114	65.8	.155	+14.7	+11.4	62	50	7.9	5.1	20.5	37.8
11.30-12.30	71.7	.123	64.7	.161	+16.0	+11.7	60	52	8.2	5.5	20.7	39.5
12.30-13.30	69.8	.133	64.4	.163	+16.9	+12.0	59	54	8.4	5.8	20.1	37.0
13.30-14.30	67.9	.143	64.4	.163	+17.6	+11.8	57	56	8.5	5.9	20.8	37.8
14.30-15.30	67.7	.145	65.4	.157	+18.2	+12.3	55	56	8.6	6.1	21.9	26.4
15.30-16.30	68.4	.140	66.7	.150	+18.4	+12.2	55	55	8.7	5.9	25.8	23.8
16.30-17.30	67.9	.143	68.0	.143	+18.6	+11.2	56	55	9.0	5.5	25.9	22.2
17.30-18.30	67.2	.147	67.5	.145	+18.2	+11.3	55	54	8.5	5.5	26.4	21.8
18.30-19.30	68.2	.142	67.5	.145	+17.3	+10.2	58	56	8.6	5.3	25.9	20.6
19.30-20.30	68.8	.138	67.8	.144	+15.7	+ 9.2	61	58	8.1	5.2	25.4	20.5
20.30-21.30	70.1	.132	68.4	.141	+13.3	+ 8.8	70	59	8.1	5.1	19.8	19.3
21.30-22.30	70.1	.132	68.6	.140	+11.5	+ 9.6	76	57	7.8	5.3	18.7	18.6
22.30-23.30	69.5	.135	68.2	.141	+10.4	+ 9.5	80	58	7.7	5.3	17.4	17.2
23.30-00.30	69.6	.134	67.2	.147	+ 9.3	+ 9.4	83	60	7.5	5.5	19.7	19.2
00.30-01.30	69.6	.134	66.4	.152	+ 8.7	+ 9.2	88	61	7.6	5.4	16.0	18.2
01.30-02.30	69.1	.137	66.0	.154	+ 8.2	+10.5	90	57	7.5	5.5	15.0	20.9
02.30-03.30	69.3	.136	67.5	.145	+ 7.8	+11.2	91	53	7.5	5.3	16.1	20.9
03.30-04.30	69.1	.137	66.5	.151	+ 7.5	+11.1	93	51	7.5	5.2	12.7	20.9
04.30-05.30	68.8	.138	66.0	.154	+ 7.0	+11.8	94	51	7.2	5.4	12.5	18.2
05.30-06.30	68.2	.142	65.7	.156	+ 8.7	+13.9	96	49	8.3	5.9	13.5	18.7
06.30-07.30	68.0	.133	64.7	.161	+11.5	+15.0	90	47	9.3	6.1	19.1	19.2
07.30-08.30	68.4	.141	64.3	.163	+14.7	+15.3	78	48	9.8	6.2	22.4	19.8

Table 7: Transmission and meteorological data from 08 September, 1981

Time	τ_{IR}	σ_{IR}	τ_{VIS}	σ_{VIS}	t (^{o}C)		RH (%)		a(g/m^{3})		V (km)	
CET	%	km^{-1}	%	km^{-1}	G	K	G	K	G	K	G	W
09.00-09.30	65.6	.156	66.1	.155	+15.7	+15.3	75	41	10.0	5.4	23.8	23.8
09.30-10.30	63.4	.169	61.8	.178	+18.0	+15.7	61	41	9.4	5.5	28.0	23.9
10.30-11.30	62.5	.174	58.4	.199	+19.7	+15.4	52	41	8.8	5.3	30.9	26.1
11.30-12.30	64.6	.162	58.4	.199	+20.4	+16.2	47	40	8.4	5.6	34.9	26.5
12.30-13.30	62.7	.173	50.4	.254	+21.1	+16.4	46	41	8.5	5.7	30.2	26.3
13.30-14.30	64.2	.164	50.0	.257	+22.0	+15.8	44	43	8.5	5.7	28.8	29.4
14.30-15.30	61.0	.183	44.9	.297	+21.5	+14.8	48	50	9.1	6.4	21.0	24.9
15.30-16.30	59.0	.196	41.6	.325	+21.1	+13.8	52	56	9.5	6.6	18.6	17.1
16.30-17.30	57.0	.208	41.5	.326	+20.2	+13.0	55	60	9.7	6.8	15.7	16.0
17.30-18.00	57.6	.205	42.8	.314	+18.6	+12.5	62	62	9.9	6.8	13.8	10.6

Table 8: Transmission and meteorological data from 04 November, 1981

Time	τ_{IR}	σ_{IR}	τ_{VIS}	σ_{VIS}	t (^{o}C)		RH (%)		a(g/m^3)		V (km)	
CET	%	km^{-1}	%	km^{-1}	G	K	G	K	G	K	G	W
07.00-07.30	75.2	.109	95.9	.0156	+ 2.6	+ 8.0	89	37	5.1	3.0	>40	>100
07.30-08.30	74.8	.108	95.9	.0156	+ 2.3	+10.3	89	35	5.0	3.4	>40	>100
08.30-09.30	76.5	.099	96.2	.0142	+ 3.0	+12.0	91	32	5.4	3.4	>40	>100
09.30-10.30	79.1	.087	96.0	.0150	+ 7.7	+12.8	91	30	7.4	3.4	>40	>100
10.30-11.14	78.1	.092	95.4	.0174	+11.4	+11.5	72	30	7.4	3.1	>40	>100
13.00-13.30	76.5	.099	92.8	.0277	+15.6	+10.7	50	36	6.6	3.5	38	>100
13.30-14.30	74.9	.107	91.8	.0319	+16.1	+ 9.4	46	40	6.3	3.6	38	>100
14.30-15.30	73.0	.117	92.8	.0277	+15.3	+ 8.9	51	52	6.6	4.3	40	>100
15.30-16.30	72.1	.121	92.8	.0277	+14.1	+ 6.9	56	58	6.8	4.5	39	>100
16.30-17.30	72.7	.118	92.5	.0290	+11.4	+ 6.2	61	60	6.3	4.4	38	>100
17.30-18.30	71.4	.124	93.1	.0266	+ 8.5	+ 5.6	73	61	6.2	4.3	34	90
18.30-19.30	71.1	.126	93.6	.0245	+ 6.5	+ 5.7	78	60	5.9	4.2	39	86
19.30-20.30	71.3	.125	93.8	.0237	+ 5.5	+ 5.6	82	58	5.8	4.1	38	80
20.30-21.30	71.5	.124	93.1	.0265	+ 4.9	+ 5.6	86	59	5.8	4.2	30	72
21.30-22.00	71.0	.127	92.8	.0277	+ 4.3	+ 5.6	88	57	5.7	4.1	23	66

Table 9: measured true extinction coefficients in stratus

σ_{IR}, σ_{VIS} = extinction coefficients in km^{-1} in the infrared and visible range

d = cloud thickness along the transmission path in m as measured by lidar

Date	Time (CET)	d	σ_{IR}	σ_{VIS}	σ_{IR}/σ_{VIS}
17.02.81	16.53	625	4.04	---	---
"	17.01	590	3.96	---	---
"	17.05	545	2.95	---	---
"	17.10	270	3.64	---	---
"	17.15	270	3.36	---	---
"	17.20	290	2.46	12.0	0.205
"	17.25	290	2.76	15.8	0.175
"	17.30	280	2.09	13.6	0.154
"	17.35	250	2.85	16.3	0.175
"	17.40	290	3.14	15.9	0.198
"	17.45	290	3.14	16.5	0.190
25.02.81	16.00	515	9.1	---	---
03.11.81	08.35	400	4.3	9.0	0.48

FIGURES

1 - 8

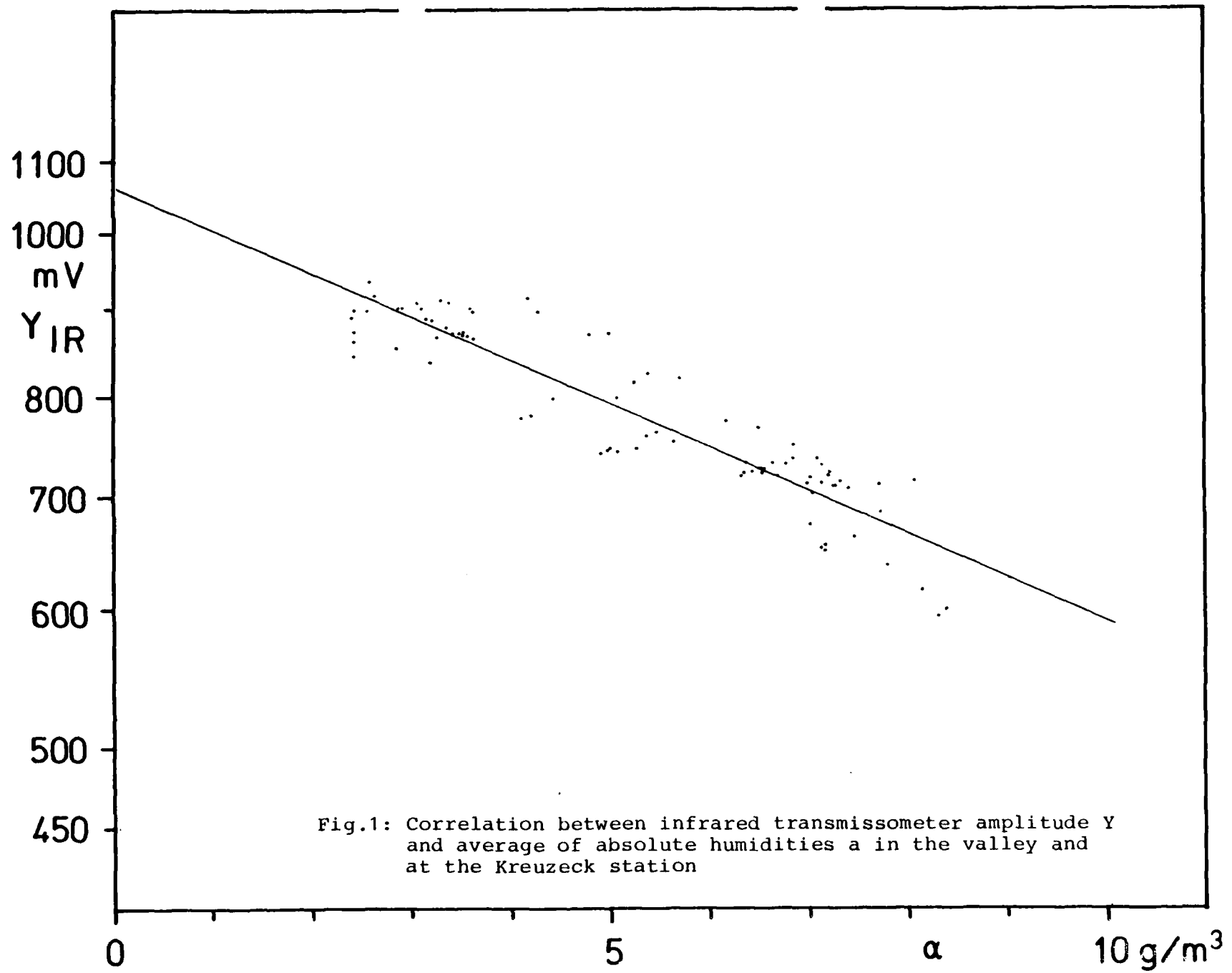

Fig.1: Correlation between infrared transmissometer amplitude Y and average of absolute humidities a in the valley and at the Kreuzeck station

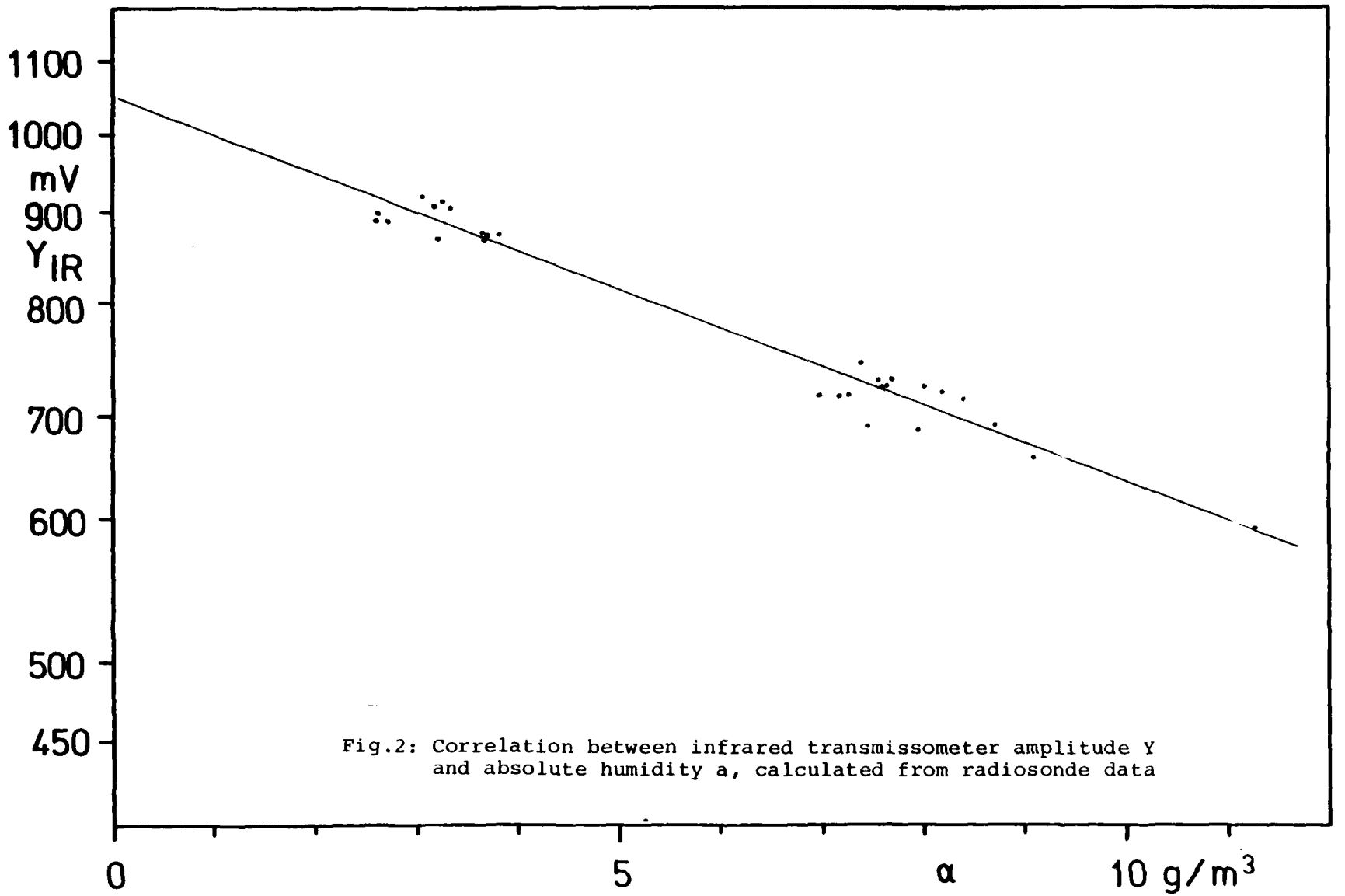

Fig.2: Correlation between infrared transmissometer amplitude Y and absolute humidity a, calculated from radiosonde data

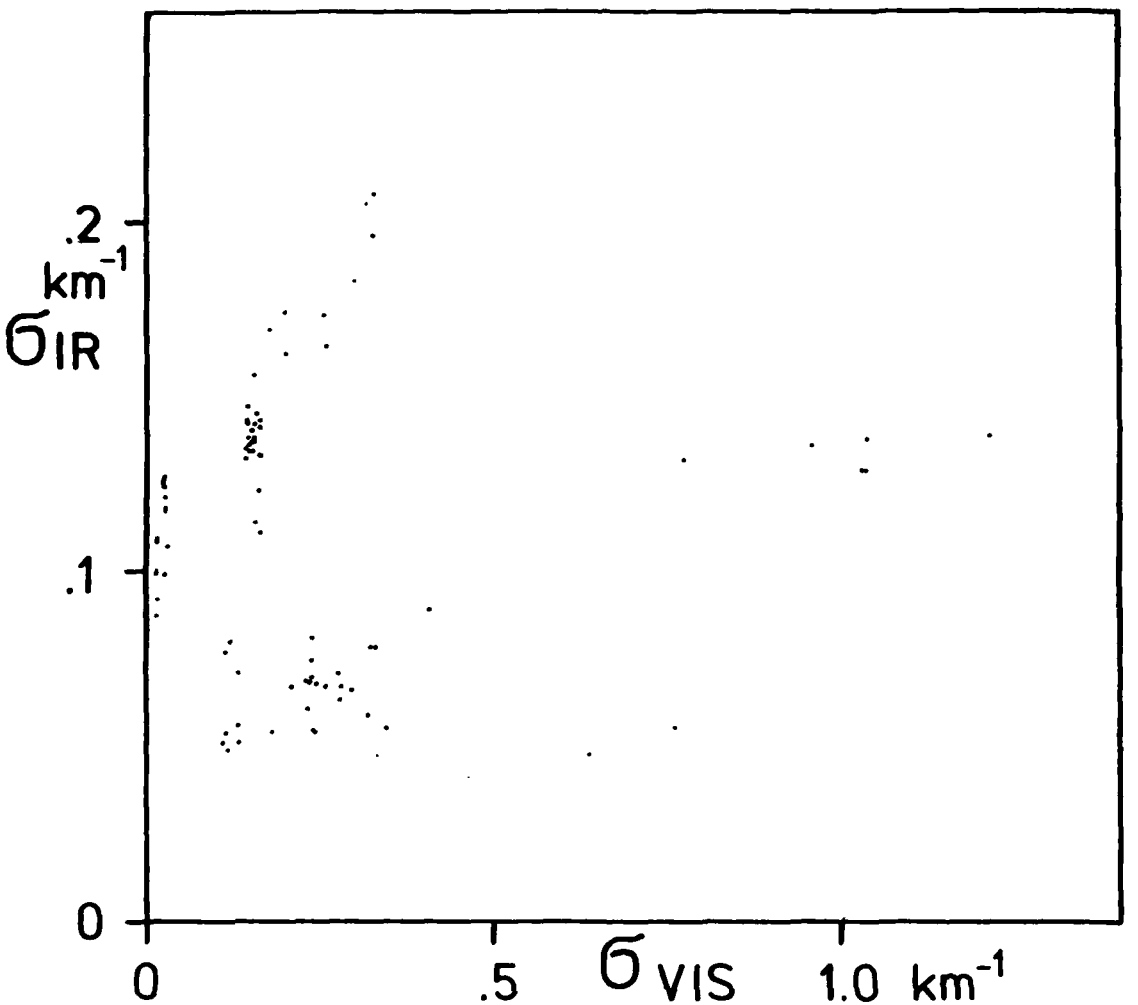

Fig.3: Correlation between infrared (σ_{IR}) and visible (σ_{VIS}) extinction coefficients under absence of clouds and precipitation

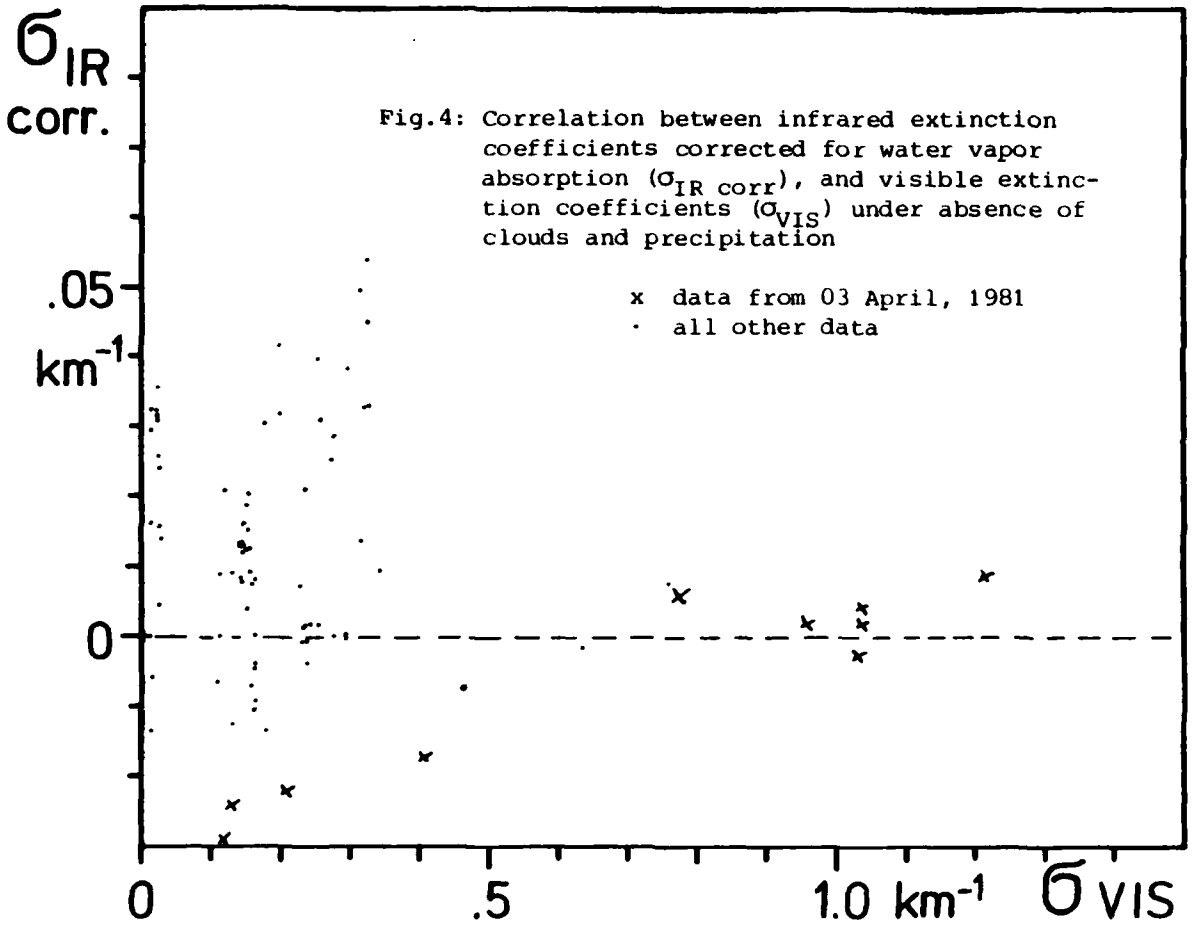

Fig.4: Correlation between infrared extinction coefficients corrected for water vapor absorption ($\sigma_{IR\ corr}$), and visible extinction coefficients (σ_{VIS}) under absence of clouds and precipitation

x data from 03 April, 1981
· all other data

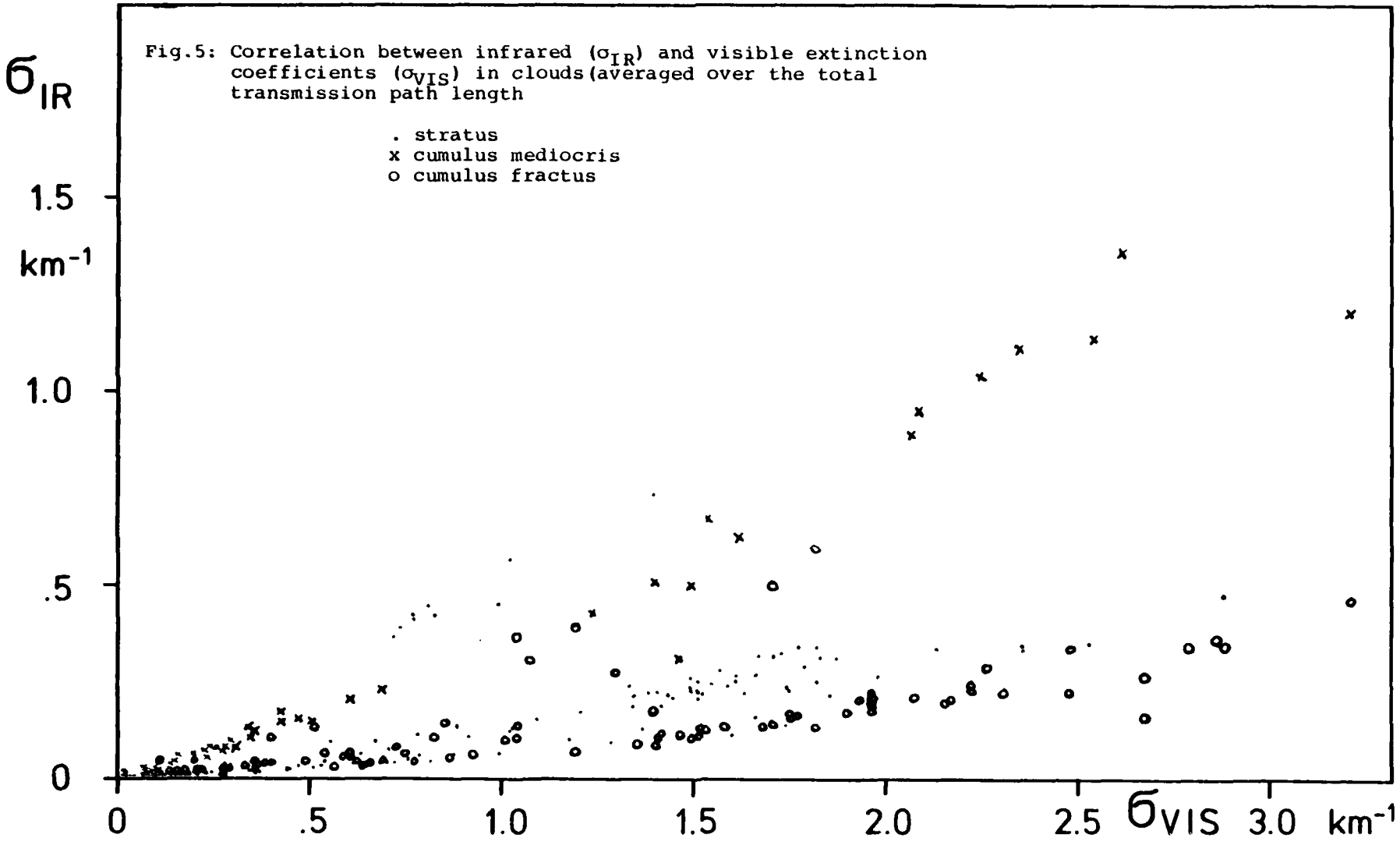
Fig.5: Correlation between infrared (σ_{IR}) and visible extinction coefficients (σ_{VIS}) in clouds (averaged over the total transmission path length
. stratus
x cumulus mediocris
o cumulus fractus
σ_{IR}
1.5
km^{-1}
1.0
.5
0
0
.5
1.0
1.5
2.0
2.5
σ_{VIS}
3.0
km^{-1}

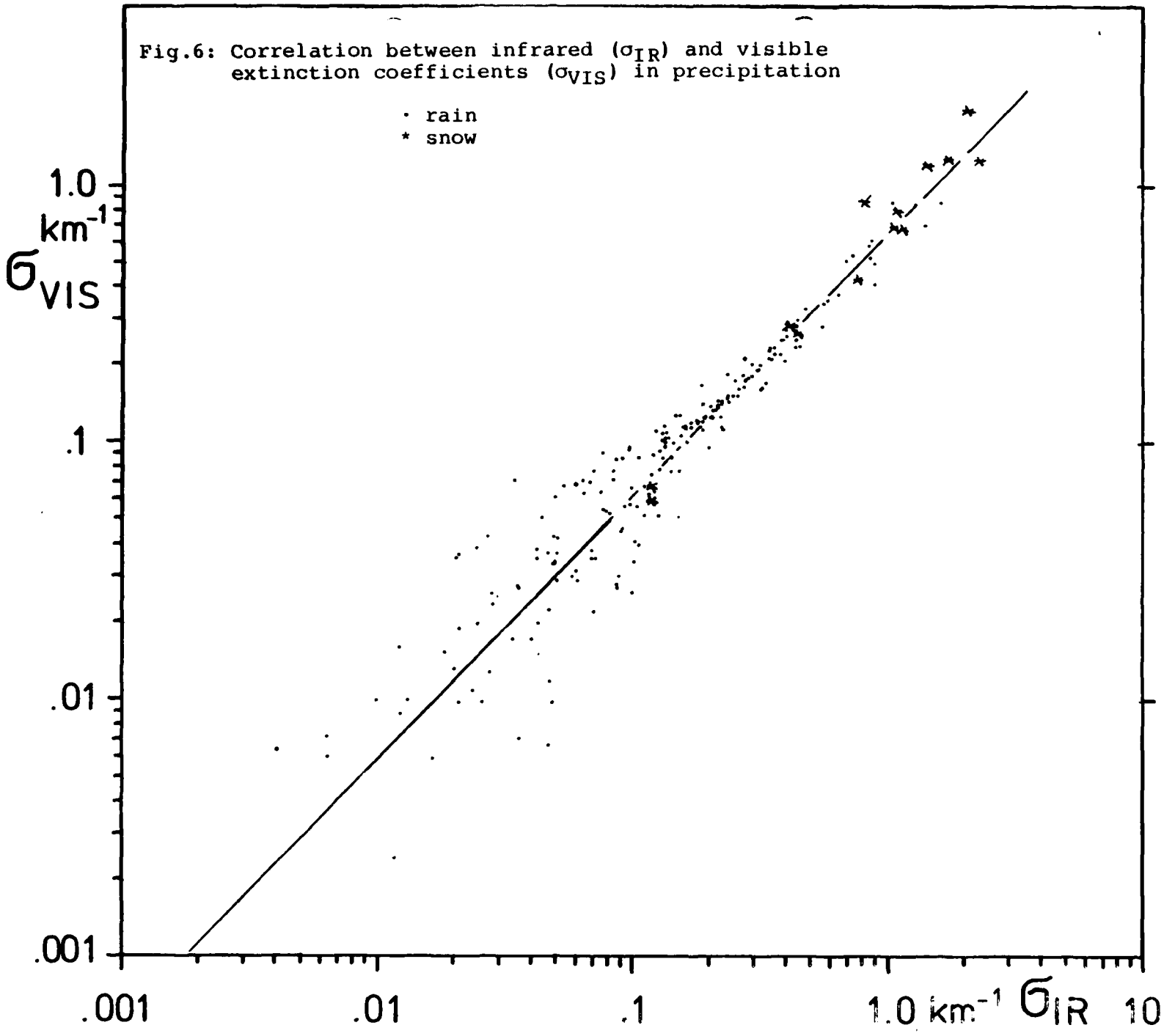
Fig.6: Correlation between infrared (σ_{IR}) and visible extinction coefficients (σ_{VIS}) in precipitation
· rain
* snow
1.0
km⁻¹
σVIS
.1
.01
.001
.001
.01
.1
1.0 km⁻¹ σIR
10

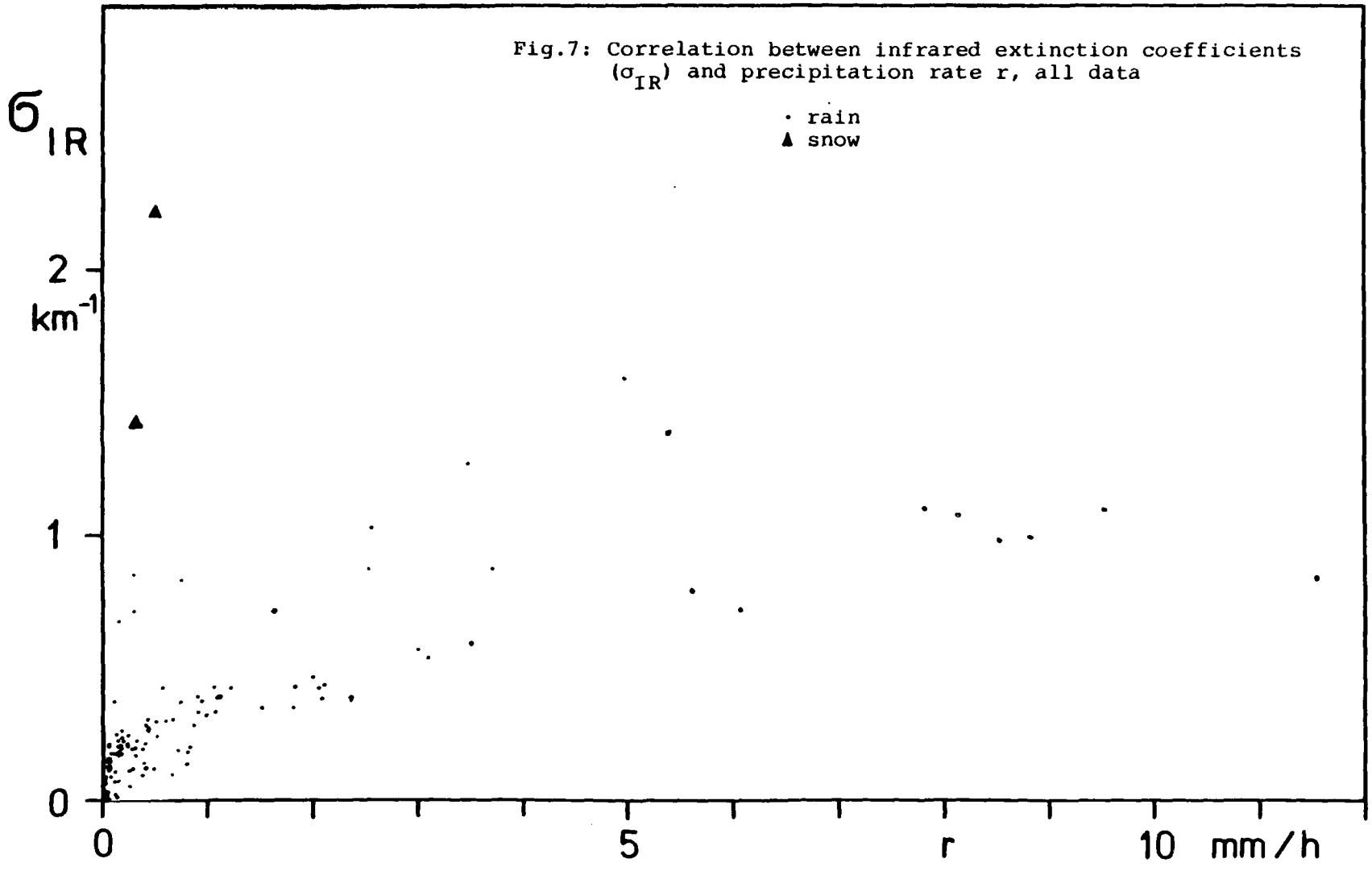

Fig.7: Correlation between infrared extinction coefficients (σ_{IR}) and precipitation rate r, all data

· rain
▲ snow

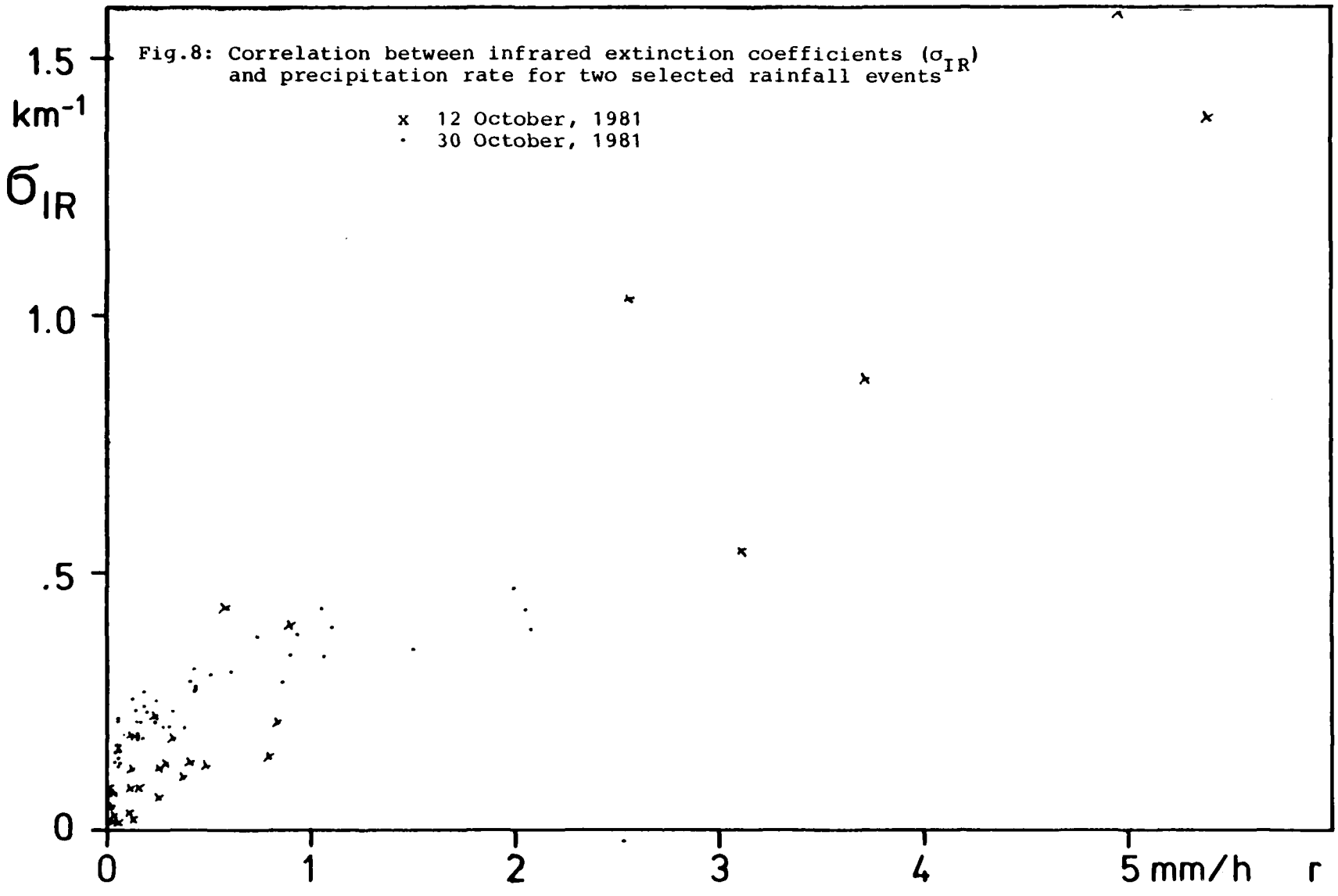

Fig.8: Correlation between infrared extinction coefficients (σ_{IR}) and precipitation rate for two selected rainfall events

x 12 October, 1981
· 30 October, 1981

END

DATE
FILMED

07-82

DTIC